

# On the Resolution of the Time-Like Singularities in Reissner-Nordström and Negative-Mass Schwarzschild

---

Amit Giveon\*, Barak Kol\*, Amos Ori†, Amit Sever\*

*\*Racah Institute of Physics*

*The Hebrew University*

*Jerusalem 91904*

*Israel*

giveon, barak\_kol, asever @phys.huji.ac.il

*†Department of Physics*

*Technion-Israel Institute of Technology*

*Haiifa 32000*

*Israel*

amos@physics.technion.ac.il

ABSTRACT: Certain time-like singularities are shown to be resolved already in classical General Relativity once one passes from particle probes to scalar waves. The time evolution can be defined uniquely and some general conditions for that are formulated. The Reissner-Nordström singularity allows for communication through the singularity and can be termed “beam splitter” since the transmission probability of a suitably prepared high energy wave packet is 25%. The high frequency dependence of the cross section is  $\omega^{-4/3}$ . However, smooth geometries arbitrarily close to the singular one require a finite amount of negative energy matter. The negative-mass Schwarzschild has a qualitatively different resolution interpreted to be fully reflecting. These 4d results are similar to the 2d black hole and are generalized to an arbitrary dimension  $d > 4$ .

---

## Contents

<b>1. Introduction</b>	<b>2</b>
<b>2. Review of the Reissner-Nordström and Schwarzschild backgrounds</b>	<b>5</b>
<b>3. Waves are smooth</b>	<b>13</b>
3.1 Set-up	13
3.2 Separation of variables	14
3.3 Normal form of the radial equation	18
3.4 Characteristic formulation	20
<b>4. Transmission cross section in Reissner-Nordström</b>	<b>21</b>
4.1 General features of the effective potential	21
4.2 Amplitudes at high energy and fixed $l$	22
4.3 Summing over $l$	24
<b>5. Generalizing the backgrounds</b>	<b>27</b>
5.1 Higher dimensions	27
5.2 The 2d black hole	29
<b>6. Adding perturbations</b>	<b>32</b>
6.1 Mass and charge	33
6.2 Interactions	33
6.3 Back-reaction for RN in $d \geq 4$	34
6.4 Back-reaction for the 2d black-hole	35
<b>7. General conditions for resolution of a singularity</b>	<b>36</b>
7.1 Uniqueness of decomposition and natural boundary conditions	36
7.2 General conditions for wave-regularity	39
<b>8. Summary and discussion</b>	<b>40</b>
<b>A. Kruskal-Szekeres coordinates</b>	<b>42</b>
<b>B. Regular singularities of ordinary differential equations</b>	<b>43</b>
<b>C. Basis functions for the characteristic formulation</b>	<b>44</b>
<b>D. Bessel functions</b>	<b>45</b>

## 1. Introduction

The importance of singularities in General Relativity and their resolution is well appreciated. The most intriguing ones are considered to be those inside black holes, and the Big-Bang-like cosmological singularities. String theory offers some cases where a time-like singularity gets resolved: the orbifold, the flop, and the conifold. These are all singularities in compact factors of spacetime, the last two occurring in Calabi-Yau manifolds, and their resolution often involves adding light matter (“twisted sectors,” “wrapped D-branes”) which lives on the singularity (for a review, see [1] and references therein). Recently, there was a renewed effort to include time-dependence in string theory (for a review, see [2] and references therein). Ultimately, one would like to understand space-like singularities such as Schwarzschild and cosmological singularities, but it would be fair to say that there were no breakthroughs yet.

The study described here was motivated by bold attempts to cross the singularity in a stringy black-hole model. The 2d black hole is a case where an algebraic coset construction requires one to add to spacetime additional manifolds which are glued together over the singularity (see figures 2,4). For the uncharged 2d black hole it was found [3] that waves sent from the “additional” infinity are fully reflected, while a charged 2d black hole does have a non-zero transmission amplitude across the singularity and, moreover, wave functions are smooth there [4].

Here we show that there is nothing intrinsically stringy in those calculations <sup>1</sup>. Actually this interesting phenomenon happens once one considers the wave equation on this background, namely, by passing from point-particle probes <sup>2</sup> to waves. More precisely, even though the wave equation is singular, the ordinary differential equation (ODE) obtained after separating time, and whose solutions we denote by  $\phi_\omega$ , allows for a unique, smooth continuation through the singularity. Interestingly, this property is not special to the 2d charged black hole, but it generalizes to the 4d charged Reissner-Nordström (RN) black hole, as well as to  $d > 4$  RN black-holes (moreover, for the 2d and 4d cases the relevant ODE is actually completely regular). This observation strongly suggests that the above classical RN spacetimes should be viewed as being made of two parts which are naturally connected across the singularity at  $r = 0$ . The two parts are (i)  $r > 0$  which is a usual (positive-mass) RN black hole, and (ii)  $r < 0$ , the region beyond the singularity, which is a negative-mass spacetime.

Another motivation for considering the negative- $r$  part of RN comes from the realistic astrophysical black holes, which are known to be rotating in general [5, 6, 7]. In the analytically-extended Kerr geometry (describing a stationary spinning black hole), the Boyer-Lindquist coordinate  $r$  goes smoothly from positive to negative values. The region  $r < 0$  is an asymptotically-flat universe (distinct from the original positive- $r$  external universe). There is a curvature singularity at  $r = 0$ , but this singularity is a ring rather than

---

<sup>1</sup>There are  $\alpha'$  corrections in string theory, which were computed in the 2d case. These give rise to extra phases in scattering amplitudes which vanish in the semi-classical limit.

<sup>2</sup>The usual definition of a singular spacetime is “geodesic-incompleteness,” namely, incomplete time-evolution for particle probes.

a hypersurface. A timelike geodesic heading towards  $r = 0$  will generically avoid the ring singularity, and smoothly pass “through the ring” into the negative- $r$  asymptotic region. Obviously, wave packets will also pass through the ring, though with partial reflection. Spherically-symmetric charged black holes were often considered as useful toy models for the more realistic spinning black holes, due to the remarkable similarity in the inner structure of the two black-hole types. From this perspective we may regard the RN solution analyzed here as such a simplified toy model for a spinning black hole.

Initially one would expect the time evolution of a wave to be ill-defined in the presence of a singularity since some boundary condition (b.c.) needs to be supplied there. Given the smooth and, in particular, univalued nature of the eigen-functions  $\phi_\omega(r)$  there is a natural way to formulate a unique time evolution simply by following the usual recipe: decompose any incoming wave packet into  $\phi_\omega$  and then endow each component with an  $\exp(i\omega t)$  time dependence. Since the eigen-functions  $\phi_\omega(r)$  are smooth at  $r = 0$ , it is just natural in this formulation to consider both sides of the singularity to be connected and communicating.

For negative-mass Schwarzschild the situation is different from the charged case, though our approach still provides a unique time evolution. In this case the  $r = 0$  singularity “flips” from being time-like at  $r < 0$  to space-like at  $r > 0$ , suggesting that gluing these two pieces would make little physical sense. Analyzing the wave equation suggests that indeed in the Schwarzschild case the field in the  $r < 0$  region evolves without any connection to the  $r > 0$  region. Unlike the RN case, here the eigen-functions  $\phi_\omega(r)$  generically have a log singularity, hence they cannot be extended across the singularity in a univalued fashion. Yet, a single regular  $\phi_{1\omega}(r)$  solution exists for each  $\omega$ . In this case a natural choice of boundary condition suggests itself – the so-called “regularity b.c.” – i.e. the demand that  $\phi_{1\omega}(r)$  be bounded at the singularity. Since we have a single regular solution for each  $\omega$ , any wave packet coming from infinity will have a unique decomposition into these regular functions  $\phi_{1\omega}(r)$ , and hence a unique time evolution. (This is to be contrasted with the RN case, in which there are two regular solutions for each  $\omega$ , and therefore, the time evolution depends on initial data from both sides of the singularity.) This “regularity b.c.” can be physically interpreted as a reflecting b.c. While normally one can define reflecting b.c. either by Dirichlet or by Neumann b.c. (or a mix) the “regularity b.c.” at Schwarzschild’s  $r = 0$  do not leave us such a choice <sup>3</sup>.

Thus we find *a natural way to define (scalar wave) physics in the presence of certain time-like singularities* (by “defining physics” we mean a recipe that allows to predict the time evolution in spacetime) simply by passing from particle probes to waves (we call such singularities “wave-regular”). We discuss two mechanisms: for RN we continue the space-time across the singularity allowing for cross-communication, while for negative-mass Schwarzschild the “regularity b.c.” are unique and define complete reflection.

We would like to pause to make a few comments on this picture:

- We consider this to be an important observation in the search for a resolution of black hole singularities, at least those of the time-like type. Yet, for this observation to

---

<sup>3</sup>It was found already in [8] by different methods that there exists a unique time evolution for negative-mass Schwarzschild, which is probably the same one we explicitly describe and physically interpret here.

be more than a mere curiosity it is required that several additional tests be satisfied such as regularity of higher-spin waves and regularity against various perturbations to the equations (some of which we perform).

- At the classical level there are issues of interpretation, for instance, the existence of these spacetimes or others with the relevant singularities, the observers living in them and implications to Cosmic Censorship, which we discuss in section 8.
- At the level of quantum gravity additional issues arise, including the validity of the wave equation and Hawking radiation whose discussion we defer to section 8 as well. Here we only want to stress that one should be cautious not to jump to conclusions and “legitimize” spacetimes with such singularities as possible solitons.

After reviewing the RN and Schwarzschild backgrounds in section 2, we explain our main observation in section 3. We formulate the wave evolution for arbitrary wave-packets coming from infinity (i.e. from large negative  $r$ ). However, the issue of specifying initial conditions on a spacelike hypersurface crossing the  $r = 0$  singularity becomes non-trivial and is relegated to section 7.

Once the unique evolution of the field is formulated, we are in a position to investigate scattering phenomena. In section 4 we study the physical properties of the RN singularity by computing the cross section for transmission. Even though the ODE for  $\phi_\omega$  is regular, the effective potential diverges as  $V_{\text{eff}} \sim -c/r^{*2}$  in the vicinity of the singularity, where  $r^* = r^*(r)$  is the canonical “tortoise” coordinate. Therefore, one would expect the singularity to have an effect even on incoming waves of very high energy – unlike a regular point in spacetime, which becomes “transparent” in this limit. Indeed we show that the high-energy transmission amplitude for fixed angular momentum  $l$  approaches 25% rather than 100%. In this respect the singularity behaves as a beam-splitter. Summing over  $l$  we find the high-energy dependence of the total cross section to be  $\propto \omega^{-4/3}$  where  $\omega$  is the frequency of the incoming plane wave. This behavior stands between the  $\omega^0$  dependence of absorption for a black hole with well-defined area, and the  $\omega^{-2}$  dependence of scattering off an elementary particle in field theory.

Generalizations of the backgrounds to higher dimensions and for the 2d black hole are presented in section 5. We determine the transmission amplitude and total cross-section as in the 4d case. The only significant difference is that while in 4d (and 2d) RN the variable-separated wave equation is regular, for  $d > 4$  it is singular-regular. Yet, all the solutions  $\phi_\omega(r)$  are still univalued for a continuation through the singularity. For Schwarzschild, on the other hand, there are no significant changes in passing from  $d = 4$  (and  $d = 2$ ) to  $d > 4$ . Hence, we also present the results for  $d = 4$  Schwarzschild in section 5.

Next we challenge our picture by adding various perturbations in section 6. So far we discussed only probes which were minimally-coupled scalar fields. Here we perform several perturbations: first we consider a field with both mass and charge, then we add interactions, and finally we consider the effect of back-reaction.

In section 7 we discuss some of the conditions for a general timelike singularity to be wave-regular, including the necessary constraint on initial conditions specified on a spacelike

hypersurface crossing the singularity, the uniqueness of decomposition of an incoming wave-packet, and the univalued property of the eigen-functions  $\phi_\omega$ . In section 8 we summarize and discuss the issues mentioned above, and list some open questions. Some technical details are given in the appendices.

Note that, in principle, this study could have been carried out a long time ago and, indeed, it turns out that there were some attempts in this direction. However, it seems that none took the conceptual freedom to cross the singularity and that actually led several authors to pronounce RN to be wave-singular. Wald [9] gave a general discussion on extending the definition of the wave equation to include non globally-hyperbolic spacetimes relying on the mathematical notion of the ‘‘Friedrichs extension.’’ Horowitz and Marolf [10] showed that some dilatonic black holes are wave-regular, where they consider a Schrödinger-like equation rather than the wave equation and demonstrate ‘‘essentially self-adjointness’’ of the associated operator. Ishibashi and Hosoya [8] were able to claim wave-regularity for negative-mass Schwarzschild by going back to the wave equation together with changing the metric in function space accordingly from the ordinary  $L^2$ -metric to the Sobolev metric, but using the same criterion of ‘‘essentially self-adjointness.’’ However, they do not comment on the physical nature of this resolution. Related work also appears in [11]. Finally, Jacobson [12] observed in passing the regularity of the time-separated wave equation near the RN singularity while studying the semiclassical decay of near-extremal black holes.

**Note added at second version:** it is interesting to consider smooth approximations to the singular geometries. We found that if one smoothly approximates the RN singularity one is required to add a finite amount of negative energy matter, which is what one would expect due to the wormhole nature of the singularity region. The details of the calculation are given in section 2 in the part titled ‘‘Negative-energy content of the smeared singularity.’’ The subsequent ‘‘perspectives on the  $r < 0$  region’’ part in section 2 as well as the discussion section should be read with this additional fact in mind. We gratefully acknowledge the valuable comments of G. Gibbons and J. Katz on this matter. See [13, 14] for a closely related case.

## 2. Review of the Reissner-Nordström and Schwarzschild backgrounds

### *Basic features of the Reissner-Nordström geometry*

The background we wish to consider is the Reissner-Nordström (RN) geometry [15, 16]. In Schwarzschild coordinates  $(t, r, \theta, \varphi)$  the metric is

$$ds^2 = -f dt^2 + f^{-1} dr^2 + r^2 d\Omega^2, \quad (2.1)$$

where

$$f = 1 - \frac{2M}{r} + \frac{Q^2}{r^2}$$

and  $d\Omega^2$  is the two-sphere metric,

$$d\Omega^2 = d\theta^2 + \sin^2 \theta d\varphi^2.$$

The electromagnetic four-potential is given by <sup>4</sup>

$$A = -\frac{Q}{r} dt .$$

For  $Q = 0$  the metric reduces to the Schwarzschild metric [17].

For the (under-extremal) non-extremal black-hole case,  $M > |Q| > 0$   $f$  has two positive roots, located at

$$r_{\pm} = M \pm \sqrt{M^2 - Q^2}.$$

Both  $r = r_+$  and  $r = r_-$  are null hypersurfaces, known as the event horizon and the inner horizon, respectively (in Schwarzschild there is only one such root,  $r = r_0 := 2M$ , which is the event horizon). Note that the roles of  $r$  and  $t$  as space-like and time-like coordinates interchange at each root of  $f$ .

The line element (2.1) is singular at the horizons, but this is merely a coordinate singularity which may be removed by transforming to other coordinates (e.g. the Kruskal-Szekeres coordinates discussed below). On the other hand,  $r = 0$  is a true physical singularity (e.g. the Ricci scalar diverges in the RN case), and we focus on this singularity in the present paper.

Usually one considers only the  $r > 0$  part of the RN geometry to be physical, but *we will find it natural to consider the  $r < 0$  region as well*. Note a crucial difference in this regard between the  $r = 0$  singularities in Reissner-Nordström and in Schwarzschild: in Reissner-Nordström  $f$  has a second-order pole at  $r = 0$ ,

$$f \cong \frac{Q^2}{r^2}, \tag{2.2}$$

and the  $t$  coordinate is time-like on both sides of  $r = 0$ , while in Schwarzschild  $f$  has a first-order pole

$$f \cong -\frac{2M}{r} \tag{2.3}$$

and the coordinates “flip” their space-like/time-like nature:  $t$  is space-like for small and positive  $r$  and it is time-like for negative  $r$ . For this reason (as well as for other reasons), we will later find it natural to glue the positive- $r$  and negative- $r$  patches of Reissner-Nordström over the singularity, but not in the Schwarzschild case. The Penrose diagram of the maximally extended Reissner-Nordström spacetime, including the  $r < 0$  region, is given in figure 2. This is to be contrasted with figure 4 which provides the Penrose diagrams of the regions  $r > 0$  and  $r < 0$  in the Schwarzschild case. These diagrams – and particularly the fact that the singularity is spacelike at  $r > 0$  and timelike at  $r < 0$  – indicate the difficulty of matching the two regions at  $r = 0$ .

### *Kruskal-Szekeres coordinates*

Although the Schwarzschild coordinates are perfectly suitable for describing the  $r < 0$  region and its matching to  $r > 0$ , insight into the “completed Penrose diagram” may be

---

<sup>4</sup>The minus sign was entered in order to conform with the rest of our sign conventions and to produce (2.19) correctly.

achieved by using the Kruskal-Szekeres coordinates, as we now describe. (In a first reading one may skip the text and only view the completed Penrose diagrams).

The  $(r, t)$  coordinates (or ‘‘Schwarzschild coordinates’’) define several metric patches, which are separated on the  $r$  axis by  $r = 0, r_-, r_+$  in Reissner-Nordström and  $r = 0, r_0$  in Schwarzschild. In order to see how these patches, and especially the  $r < 0$  patch, are connected one transforms to the Kruskal-Szekeres coordinates [18, 19], and later performs a conformal transformation to obtain the Penrose diagram (in appendix A we review the procedure). Here again we will find a qualitative difference between the Reissner-Nordström singularity and Schwarzschild.

In Kruskal-Szekeres coordinates  $(U, V)$ , one uses a function  $g(r)$  to implicitly define  $r$  through

$$-UV = g(r) . \quad (2.4)$$

This function is defined by

$$g(r) := \exp(\pm 2 \kappa r^*) , \quad (2.5)$$

in terms of the ‘‘tortoise’’ coordinate  $r^*$ :

$$dr^* := \frac{dr}{f} . \quad (2.6)$$

$\kappa$  is the surface gravity of the relevant horizon and the choice of sign is correlated with the choice of sign for  $U$  and  $V$ .

Let us look at the functions  $g(r)$ . For RN  $g_{\pm}(r)$  are given by (see figure 1)

$$\begin{aligned} g_+(r) &= \left( \frac{r}{r_+} - 1 \right) \left( \frac{r}{r_-} - 1 \right)^{-\frac{\kappa_+}{\kappa_-}} \exp(2 \kappa_+ r) \\ g_-(r) &= \left( 1 - \frac{r}{r_-} \right) \left( 1 - \frac{r}{r_+} \right)^{-\frac{\kappa_-}{\kappa_+}} \exp(-2 \kappa_- r) \end{aligned} \quad (2.7)$$

where  $g_+$  covers the ‘‘plus plane’’ which includes the outer horizon at  $r_+$  :  $r_- < r < \infty$ , and  $g_-$  covers the ‘‘minus plane’’ including the inner horizon at  $r_-$  :  $-\infty < r < r_+$ . From the form of  $g_-$  one realizes that in these coordinates the  $r < 0$  region is naturally included and it lies at  $(-U_- V_-) > 1$ , which is adjacent to the  $0 < r < r_-$  or  $0 < -U_- V_- < 1$  region, and as such we include it in the Penrose diagram (figure 2).

For Schwarzschild on the other hand, we have

$$g_{\text{schw}}(r) = \left( \frac{r}{r_0} - 1 \right) \exp(r/r_0). \quad (2.8)$$

One notes that unlike the  $g_{\pm}$  which were monotonic  $g_{\text{schw}}(r)$  has a minimum at  $g_{\text{schw}}(r = 0) = -1$  (see figure 3), exactly because  $f_{\text{schw}}(r)$  changes sign at 0. Thus for  $-UV < -1$  there is no solution for  $r$  while in the region  $-1 < -UV < 0$  there are two solutions one of them with negative  $r$ . Hence, the  $r < 0$  region is naturally included and becomes a second cover over the inside of the black hole ( $0 < r < r_0$ ) which we incorporate into the Penrose diagram in figure 4. This second cover differs from Reissner-Nordström where the  $r < 0$  region was located side by side with the ‘‘ordinary’’  $r > 0$  regions. This difference



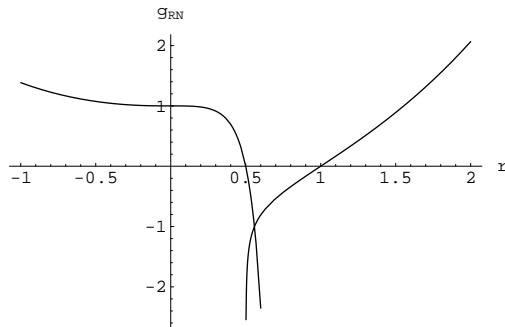


**Figure 1:** The two functions  $g_{\pm}(r)$  which determine  $r$  in Kruskal-Szekeres coordinates for Reissner-Nordström implicitly through  $-U_{\pm} V_{\pm} = g_{\pm}(r)$ .  $g_+$  is defined for the  $r > r_-$ , namely on the plus plane, and  $g_-$  is defined on  $r < r_+$  namely on the minus plane. Note that both functions are monotonic with range  $(-\infty, +\infty)$  and hence there is always a unique solution for  $r$ . For  $(-U_- V_-) > 1$  on the minus plane  $r$  is negative. In drawing the figure the values  $r_- = .5$ ,  $r_+ = 1$  were used.

is in tune with our later conclusion that for Reissner-Nordström one should glue the two regions over the  $r = 0$  singularity while in Schwarzschild they should be considered to be disconnected.

#### *Negative-energy content of the smeared singularity*

The electro-vacuum geometry constructed here has a curvature singularity at  $r = 0$ . One may consider modifying the metric function in the very neighborhood of  $r = 0$ , say at some  $|r| \leq r_0$ , so as to make the geometry smooth. In this way one obtains a wormhole smoothly connecting the positive- $r$  and the negative- $r$  parts. However, any such smearing will imply the presence of additional energy-momentum in the region  $|r| \leq r_0$ , as would be determined by applying the Einstein operator to the modified metric. The specific form of the additional energy-momentum tensor will depend on the specific choice of smearing. It is well known, however, that any wormhole of this kind requires “exotic” matter fields, i.e. an energy-momentum source which violates the weak energy condition. A simple way to understand it is to consider a congruence of null rays propagating inward radially. In this setting Raychaudhuri’s equation tells us that as long as the energy condition is satisfied  $\frac{d^2}{d\lambda^2} \log(A) \leq 0$ , where  $A$  is the transverse area (of the two-sphere) and  $\lambda$  is an affine parameter along the ray. Since  $A$  (and  $\log(A)$ ) is asymptotically decreasing in an inward radial motion, but after going through the “wormhole” it is again increasing, there must be an intermediate region where the weak energy condition is violated.

We wish to evaluate the amount of negative energy required to support this wormhole-shaped smeared geometry, particularly at the limit  $r_0 \rightarrow 0$ . To be more specific, we consider here a thin-shell model [20]. Namely, we directly match the geometry at  $r \geq r_0$  to that at  $r \leq -r_0$ , through a thin shell located at  $|r| = r_0$ , for some  $0 < r_0 \ll Q$ . This thin shell is a timelike hypersurface parameterized by the three coordinates  $(t, \theta, \varphi)$ . Note that the induced three-geometry is continuous across this shell:  $g_{\theta\theta}$  and  $g_{\varphi\varphi}$  only depend on  $r^2$ , and  $g_{tt}$  (which originally has different values at the two sides) becomes continuous after a

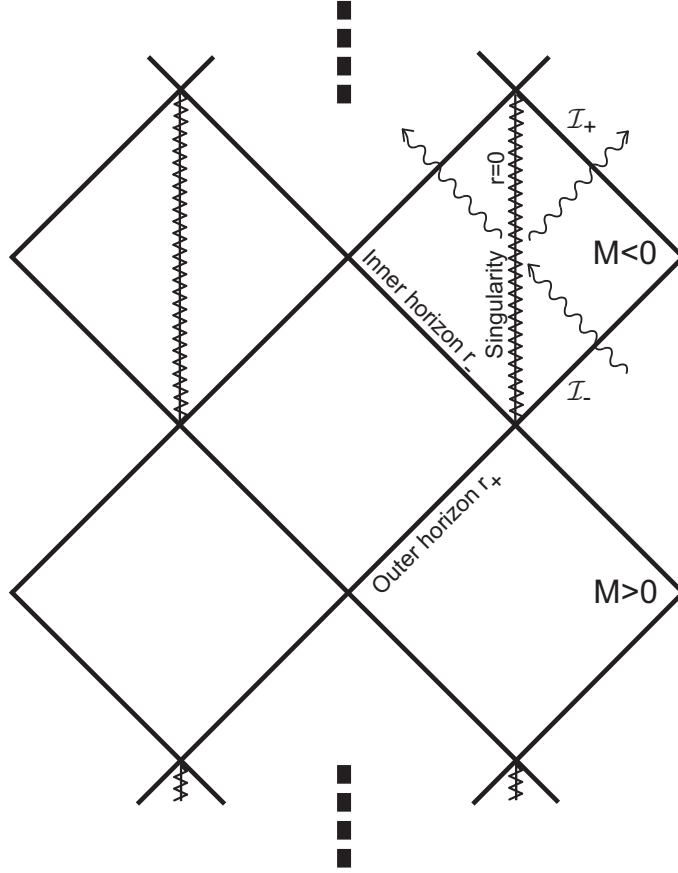


**Figure 2:** The complete Penrose diagram for the (under-extremal  $|Q| < |M|$ ) Reissner-Nordström background including the regions with  $r < 0$  which are not drawn usually. These regions are glued to “the other side” of the time-like singularity, which is seen as naked from that side. The wavy lines denote a typical scattering experiment off the singularity. Waves from  $\mathcal{I}^-$  are sent to the singularity. Some of them are reflected back to  $\mathcal{I}^+$  while the remainder is transmitted to  $r > 0$ .

trivial rescaling of the  $t$  coordinate at e.g.  $r < -r_0$ .

The shell’s contribution to the energy-momentum tensor may be expressed as [21]

$$T^{\mu\nu}(x) = S^{\mu\nu}(x)\delta(\eta) , \quad (2.9)$$

where  $S^{\mu\nu}$  is the shell’s surface energy-momentum distribution, and  $\eta$  is the proper-length parameter along radial lines of constant  $t, \theta, \varphi$ , with  $\eta = 0$  at the shell and  $\eta > 0$  at  $r > r_0$ . The surface distribution  $S^{\mu\nu}$  is determined from the jump in the extrinsic curvature,

$$S_j^i = -\frac{1}{8\pi} \left( \langle K \rangle_j^i - \delta_j^i \langle K \rangle_k^k \right). \quad (2.10)$$

Hereafter  $i, j, k$  run over the three coordinates  $(t, \theta, \varphi)$ , and

$$\langle K \rangle_j^i \equiv K_j^{i(+)} - K_j^{i(-)}, \quad (2.11)$$

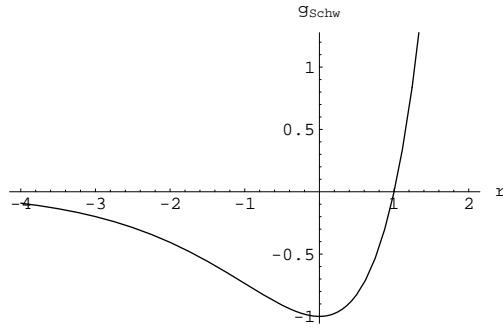


**Figure 3:** The function  $g_{\text{schw}}(r)$  which determines  $r$  in Kruskal-Szekeres coordinates (for the Schwarzschild black hole) implicitly through  $-UV = g_{\text{schw}}(r)$ . Note that while for  $g_{\text{schw}} > 0$  there is a unique solution for  $r$ , for  $-1 < g_{\text{schw}} < 0$  there are two solutions, one of them with negative  $r$  which lead to a double cover in Kruskal-Szekeres coordinates. Finally for  $g_{\text{schw}} < -1$  there are no solutions.

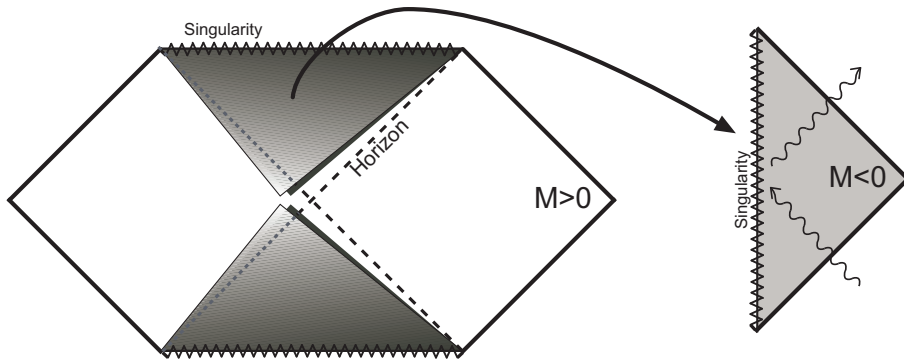


**Figure 4:** The complete Penrose diagram for a Schwarzschild black hole including the negative-mass regions which appear as a double cover of the inside of the black (or white) hole. The negative-mass regions are shown separately on the side, rotated by 90 degrees so that time flows in them upward as is conventional. Here we will find no communication through the singularity.

where  $K_j^{i(\pm)}$  is the shell's extrinsic curvature with respect to the geometries at  $r > r_0$  and  $r < -r_0$ , respectively. (We are using here General-Relativistic units,  $G = c = 1$ .) The extrinsic curvature may conveniently be expressed in terms of Israel's “natural coordinates” [20], which we take here to be the three hypersurface coordinates  $t, \theta, \varphi$  and the above proper-length coordinate  $\eta$ :

$$K_{ij}^{(\pm)} = \frac{1}{2} \left[ \frac{\partial g_{ij}}{\partial \eta} \right]_{(\pm)} = \frac{1}{2} \left[ g_{rr}^{-1/2} \frac{\partial g_{ij}}{\partial r} \right]_{(\pm)}, \quad (2.12)$$

with the derivatives (and  $g_{rr}$ ) evaluated at the (+) or (−) sides of the shell, respectively.

We are primarily interested here in the amount of (negative) energy contributed by the shell, represented by  $S_t^t$ :

$$S_t^t = \frac{1}{8\pi} \left( \langle K \rangle_\theta^\theta + \langle K \rangle_\varphi^\varphi \right) = \frac{1}{4\pi} \langle K \rangle_\theta^\theta. \quad (2.13)$$

A straightforward application of Eq. (2.12) yields

$$K_{\theta}^{\theta(\pm)} = \left[ \frac{\sqrt{1 - 2M/r + Q^2/r^2}}{r} \right]_{r=\pm r_0}, \quad (2.14)$$

hence

$$\langle K \rangle_{\theta}^{\theta} = \frac{\sqrt{1 - 2M/r_0 + Q^2/r_0^2} + \sqrt{1 + 2M/r_0 + Q^2/r_0^2}}{r_0}. \quad (2.15)$$

Let  $\rho$  denote the shell's energy density as measured by a static observer:

$$\rho = -T_t^t = -\frac{1}{4\pi} \langle K \rangle_{\theta}^{\theta} \delta(\eta) \quad (2.16)$$

(recall that  $T_t^t$  is invariant to a rescaling of  $t$ ). The total shell's energy is obtained by integrating over the 3-volume, i.e. over  $\eta$  and over the shell's area:

$$\begin{aligned} E_{shell} &= 4\pi r_0^2 \int \rho d\eta = -r_0^2 \langle K \rangle_{\theta}^{\theta} \\ &= -r_0 \left( \sqrt{1 - 2M/r_0 + Q^2/r_0^2} + \sqrt{1 + 2M/r_0 + Q^2/r_0^2} \right). \end{aligned}$$

Finally, we calculate  $E_{shell}$  at the limit where  $r_0$  shrinks to zero:

$$E_{shell}^0 \equiv \lim_{r_0 \rightarrow 0} E_{shell} = -2Q. \quad (2.17)$$

### *Perspectives on the $r < 0$ region*

The metric (2.1) is invariant under the transformation  $r \rightarrow -r$ ,  $M \rightarrow -M$ , and hence we shall often refer to the  $r < 0$  region as the “negative mass” region. To an observer in the asymptotically-flat region at  $r < 0$  the central object will appear as one of negative mass, namely, a gravitationally-repelling object.<sup>5</sup>

We alert the reader that negative masses have very unusual features:

- A negative mass produces anti-gravity, namely it repels all masses.
- As a result of Newton's second law  $F = ma$ , the acceleration of a negative mass is reversed to the force acting on it.
- As an immediate result of the two properties above, if one were to place two bodies initially at rest, one with a negative mass and the other with a positive mass, both will accelerate in the same direction going from the negative mass to the positive one (furthermore, if the two masses are of the same magnitude, they will uniformly accelerate forever).

---

<sup>5</sup>This is also the situation in the Kerr geometry: in the asymptotically-flat region  $r < 0$  the central object is gravitationally repelling.

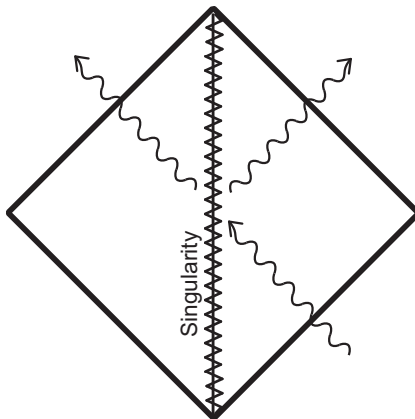


**Figure 5:** The complete Penrose diagram for an over-extremal ( $|M| < |Q|$ ) Reissner-Nordström black hole. It is composed of a positive-mass RN glued over the singularity to a negative-mass RN. There are no horizons and the singularity is naked on both sides.

Due to these unusual features (and possibly others), negative masses are often excluded (however, see [22]). We shall not attempt here to provide a conclusive answer to this question. Instead, we will take a pragmatic approach of exploration by allowing negative-mass spaces in the current context and being alert to the appearance of a problem such as a resulting inconsistency. We will not find any such inconsistency in this paper, and so we regard this question as remaining open.

In the (under extremal) RN black-hole case,  $M > |Q| > 0$ , one can reach the  $r = 0$  singularity either from the negative-mass asymptotic region (i.e. from large negative  $r$ ), or from  $r \rightarrow r_-$ , the inner horizon. Looking at the Penrose diagram of the maximally extended spacetime, figure 2, one may consider reaching the inner horizon by jumping into the black hole from the ordinary (positive-mass) asymptotic region. The inner horizon of the pure RN geometry is a perfectly-regular hypersurface. However, it is known already for some time that the inner horizon is unstable to perturbation and should become singular [23, 24] in “realistic” charged black holes. For this reason it was often believed that the inner horizon cannot be crossed. Recent investigations, however, indicated that the singularity at the inner horizon is weak, that is, the tidal forces are too weak to harm physical objects [25, 26, 27]. Therefore, there is no obvious reason to exclude objects falling into the black hole and arriving at  $r = 0$  through the inner horizon. For conceptual simplicity, however, we shall primarily consider here observers arriving at  $r = 0$  from the negative- $r$  asymptotically-flat region, namely, from beyond the singularity.

In the case  $|Q| > M$  (figure 5) there are no horizons, but simply two asymptotically-flat regions, one with positive mass and the other with negative mass (in this case there is no reason to transform into Kruskal-Szekeres -like coordinates). In both regions there is a naked singularity at  $r = 0$ , and we glue the two patches there.

### *Geodesics*

We end this section with a review of particle motion in this background, and a deriva-

tion of the effective potential for particles (or geodesics) which we later compare with the effective potential for waves. The geodesic equation for a particle of mass  $m$  can be derived from the Hamiltonian system

$$\mathcal{H} = \frac{1}{2} g^{\mu\nu} p_\mu p_\nu = -\frac{1}{2} m^2 \quad , \quad (2.18)$$

where the Hamiltonian is automatically with respect to a multiple of the proper time  $\tau$ . For a particle of charge  $q$  one replaces  $p \rightarrow p - qA$ .

Since  $\mathcal{H}$  is independent of  $t$  and  $\phi$  we have the constants of the motion  $E := -p_t$ ,  $l := p_\phi$ . The motion is then described by

$$0 = \dot{r}^2 + V_{\text{eff}}^{\text{geodesic}}(r) \quad ,$$

$$V_{\text{eff}}^{\text{geodesic}}(r) = \left( \frac{l^2}{r^2} + m^2 \right) f(r) - \left( E - \frac{qQ}{r} \right)^2 \quad . \quad (2.19)$$

In particular, around  $r \simeq 0$ ,  $V_{\text{eff}} \sim \frac{l^2 Q^2}{r^4}$  for  $l > 0$  [and  $V_{\text{eff}} \sim (m^2 - q^2) \frac{Q^2}{r^2}$  for  $l = 0$ ]. Note that the effective potential given here does not have the ordinary units of potential, but it has the advantage of being general and valid both for massive and massless particles. In order to get the physical potential in a Newtonian approximation one needs to rescale  $V_{\text{eff}}$  by an appropriate power of  $m$ .

### 3. Waves are smooth

#### 3.1 Set-up

A spacetime is usually defined to be singular when it is not geodesically complete, namely with respect to point-particle probes. Yet, all the fundamental interactions are formulated for field theories, where particles are derived concepts constructed from appropriate wave packets. Moreover, the mashing of Quantum Mechanics and Special Relativity requires the quantum theory of fields. Thus it is natural to probe spacetimes with waves rather than point-particles.

Here we will confine ourselves, as a first step, to scalar fields. Initially we will further assume a minimally-coupled free field with no mass or charge, and later these assumptions will be relaxed and shown not to affect the results.

When should we consider a spacetime to be wave-regular? A central objective of physics is to provide predictions for the results of experiments, or a well-defined time evolution, and it is exactly this predictability which is at risk in the presence of a singularity. We would therefore consider a spacetime to be wave-regular if the time evolution is unique for any physically acceptable initial conditions (to be discussed below). Technically the issue is whether one can supply boundary conditions at the singularity such that the time evolution is regular and whether these are unique.

In “normal” (i.e. non-singular) situations there are two different set-ups for initial conditions: (i) the Cauchy formulation, in which the field and its time derivative are specified on a spacelike hypersurface; and (ii) the characteristic formulation, in which

the field is specified on two null hypersurfaces. This second formulation has a special, widely used variant (iia) in which the null hypersurfaces are taken to be at the null past boundaries of the region of spacetime under consideration – e.g. past null infinity (for an asymptotically-flat region), and a past horizon (for an asymptotically-flat region outside a black hole).

In our problem – formulating the time evolution of the field at the two sides of the  $r = 0$  singularity – the Cauchy formulation (i) has a potential problem, because any spacelike initial hypersurface must cross the  $r = 0$  singularity. It is a priori unclear what are exactly the “physically-acceptable initial conditions” near  $r = 0$ . On the other hand, the characteristic formulation (ia) is free of this potential problem. The two null hypersurfaces which naturally suggest themselves for this formulation are past null infinity ( $\mathcal{I}^-$ ) of the negative- $r$  universe, and the inner horizon  $r_-$ . These two hypersurfaces nowhere intersect the singularity, or even get close to it.

We shall therefore base our analysis of time evolution on this characteristic formulation. That is, we probe the spacetime by wave-packets prepared and sent in from the asymptotic regions far away from the singularity. Indeed, it is physically reasonable to characterize the singularity by its response to any possible scattering experiment. Motivated by these considerations, we shall define a spacetime (or a region of spacetime) to be *wave-regular* if the time evolution is unique for generic initial conditions specified at the relevant past null boundaries of this (region of) spacetime.

While the characteristic formulation (ii) avoids the issue of putting constraints on initial conditions near the singularity, which is indeed non-trivial in hindsight, it does require a global point of view, whereas our resolution is essentially local. This local property is better understood in the Cauchy formulation (i) and hence we will briefly review both formulations in this section. Actually one could define also a hybrid of these methods which keeps both locality and some isolation from the singularity: namely, a formulation (ia) in which the field and its derivatives are supplied on a spacelike hypersurface but are required to vanish in a neighborhood of the singularity.<sup>6</sup>

In what follows we shall show that both the  $-\infty < r < r_-$  piece of the RN spacetime and negative-mass Schwarzschild are indeed wave-regular. We shall define first the time evolution in a straightforward manner in the Cauchy formulation, and then after defining a canonical form for the radial equation and the effective potential we shall state the characteristic formulation. A treatment of the interesting subtleties in the Cauchy formulation will be deferred to section 7.

### 3.2 Separation of variables

Let us proceed by writing down the wave equation for a minimally coupled massless scalar field  $\phi$  in the RN (or Schwarzschild) background (2.1). After separating the angular variables

$$\phi(r, t, \Omega) = \phi_l(r, t) Y_{lm}(\Omega) , \tag{3.1}$$

---

<sup>6</sup>This variant is slightly more restrictive than just a re-formulation of the initial-value setup, as it demands that the field strictly vanishes at some open neighborhood. Nevertheless it is still sufficiently general to allow for physically-meaningful scattering experiments.

where  $\Omega$  denotes the angular variables <sup>7</sup>  $(\theta, \varphi)$ , one has

$$0 = \square\phi = \left[ -f^{-1} \partial_{tt} + \frac{1}{r^2} \partial_r f r^2 \partial_r - \frac{l(l+1)}{r^2} \right] \phi_l . \quad (3.2)$$

The wave equation (3.2) is singular at  $r = 0$ : after multiplying the equation by  $f$  to extract  $\partial_{tt}$ , the part containing e.g. the second-order  $r$  derivative becomes  $f^2 \partial_{rr}$ , and  $f^2$  diverges as  $r^{-4}$ . This is not surprising since we know that  $r = 0$  is a curvature singularity.

Still, we may attempt a straight-forward separation of the time variable,

$$\phi_l(r, t) = \phi_{\omega l}(r) \exp(i \omega t) , \quad (3.3)$$

getting

$$0 = \square_{\omega l} \phi_{\omega l} \\ \square_{\omega l} := f^{-1} \omega^2 + \frac{1}{r^2} \partial_r f r^2 \partial_r - \frac{l(l+1)}{r^2} . \quad (3.4)$$

It will be convenient to normalize  $\square_{\omega l}$  in two different ways: if we want to have a unit coefficient for  $\partial_{rr}$  then we work with  $f^{-1} \square_{\omega l}$  while  $f \square_{\omega l}$  achieves a unit coefficient for  $\omega^2$ . Indeed, writing down  $f^{-1} \square_{\omega l}$  explicitly, we have

$$0 = f^{-1} \square_{\omega l} \phi_{\omega l} = \\ = \left[ \frac{1}{f r^2} \partial_r f r^2 \partial_r - \frac{l(l+1)}{f r^2} + f^{-2} \omega^2 \right] \phi_{\omega l} , \quad (3.5)$$

and at this point we need to discuss the Reissner-Nordström case and the Schwarzschild case separately.

### *Reissner-Nordström*

Since  $f_{RN} r^2 \cong Q^2$  is regular at  $r = 0$ , the variable-separated equation (3.5) is surprisingly completely regular. This observation is at the heart of our proposed resolution. To leading order it is given by

$$0 = \left[ (1 + \dots) \partial_{rr} + O(r^0) \partial_r - (1 + \dots) \frac{l(l+1)}{Q^2} + (1 + \dots) \frac{r^4}{Q^4} \omega^2 \right] \phi_{\omega} , \quad (3.6)$$

where ellipses always denote corrections which are higher order in  $r$ , and from now we will often write  $\phi_{\omega}$  instead of  $\phi_{\omega l}$  suppressing the index  $l$  for clarity. Note that the equation is not only non-singular but also analytic (namely,  $\phi_{\omega,rr}$  is an analytic function of  $\phi_{\omega}, \phi_{\omega,r}$  and  $r$ ) at  $r = 0$ , for any  $l$  and  $\omega$ .

Since all the solutions for this equation are smooth at  $r = 0$ , a natural way to define the time evolution suggests itself: given an initial wave packet (which propagates from either  $\mathcal{I}^-$  and/or the inner horizon) decompose it into radial eigen-functions  $\phi_{\omega}(r)$ . Since the eigen-functions  $\phi_{\omega}(r)$  are smooth at  $r = 0$ , the time evolution defined above will be

---

<sup>7</sup>The notation  $\Omega$  for the angular variables is convenient for the generalization to higher dimensions where there are more angular variables and there is no need to explicitly define them.



smooth there. Consequently, parts of the wave packet will cross this point. It is therefore essential to include both sides of the  $r = 0$  singularity in our analysis.

In equations: given initial conditions  $\phi_i(r) := \phi(r, t = 0)$  and  $\dot{\phi}_i(r) := \dot{\phi}(r, t = 0)$  (we chose here the initial hypersurface  $t = 0$  without loss of generality), one determines the decomposition  $\phi_+(k)$ ,  $\phi_-(k)$  that satisfies

$$\begin{aligned}\phi_i(r) &= \int (\phi_+(k) + \phi_-(k)) \phi_k(r) dk \\ \dot{\phi}_i(r) &= \int i\omega (\phi_+(k) - \phi_-(k)) \phi_k(r) dk\end{aligned}\quad (3.7)$$

where here  $\omega := |k|$ , and  $\phi_k$  denotes two independent solutions (one for positive  $k$  and one for negative  $k$ ) of the wave equation  $\square_{\omega l} = 0$  (with  $\omega = |k|$ ).<sup>8</sup> Now the time evolution is defined naturally to be<sup>9</sup>

$$\phi(r, t) = \int (\phi_+(k) \exp(+i\omega t) + \phi_-(k) \exp(-i\omega t)) \phi_k(r) dk \quad . \quad (3.8)$$

In the characteristic formulation the decomposition into modes may be done by Fourier-decomposing the waves coming from  $\mathcal{I}^-$  or from the inner horizon in  $\exp(i\omega v)$  or  $\exp(i\omega u)$ , respectively, where  $u$  and  $v$  are the two Eddington-like null coordinates, and associating a certain radial function  $\phi_\omega(r)$  with each Fourier component. This will be described in more detail in subsection 3.4.

At first it may look as if the singular partial differential equation (3.2) has turned completely regular. Later we will see, however, that some imprint of the singularity remains. This is expressed both in the unusual large- $\omega$  limit of the transmission amplitude through  $r = 0$  (see section 4) and in the constraints for Cauchy initial conditions at  $r \sim 0$  (see section 7).

### *Schwarzschild*

Using the leading behavior of  $f_{\text{Schw}}$  at  $r = 0$  (2.3), the variable-separated equation (3.5) is given to leading order by

$$0 = \left[ (1 + \dots) \partial_{rr} + \frac{(1 + \dots)}{r} \partial_r + (1 + \dots) \frac{l(l+1)}{2Mr} + (1 + \dots) \frac{r^2}{4M^2} \omega^2 \right] \phi_\omega \quad . \quad (3.9)$$

One notices that this equation is not regular anymore, but rather the  $\partial_r$  and the  $l(l+1)$  terms are singular. Actually it falls into the so called “regular-singular” category of mild singularities (see appendix B for a rudimentary review).

Looking at Eq. (3.9) one realizes that the characteristic exponents (defined by the attempted leading-order solution  $\phi_\omega \cong r^\rho$ ) are  $\rho_1 = \rho_2 = 0$ , and thus the two independent solutions behave as  $\phi_{1\omega} \sim r^0$ ,  $\phi_{2\omega} \sim \log(r)$  at  $r \sim 0$ . So unlike Reissner-Nordström one of the solutions is singular, and moreover does not have a single-valued continuation to

---

<sup>8</sup> $\phi_k$  are usually chosen such that  $\phi_k \simeq \exp(ikr^*)/r$  at large  $r^*$  (large negative  $r$ ).

<sup>9</sup>This amounts to taking the radial function  $\phi_{\omega l}(r)$  of Eq. (3.3) to be  $\phi_+(k = +\omega) + \phi_+(k = -\omega)$  for  $\omega > 0$  and  $\phi_-(k = +\omega) + \phi_-(k = -\omega)$  for  $\omega < 0$ .

negative  $r$ , and there is no sense in gluing together positive  $r$  to negative  $r$ . It is perhaps fortunate that this is the case, since gluing the two sides would require dealing with the “flip” in the nature of  $(r, t)$  from space-like to time-like (and an arbitrary choice of the direction of the arrow of time). Still we find it remarkable that one of the solutions does turn out to be regular. This half-regularity allows a natural definition of the time evolution, as we shortly describe, where this time there is no transmission through  $r = 0$ .

The situation here is analogous to the relation between a free field  $\phi$  on the infinite line  $-\infty < r < +\infty$  to a free field on the semi-infinite line  $0 < r < +\infty$ , which could be e.g. the radial coordinate in some higher dimension, with Dirichlet or Neumann boundary condition at  $r = 0$ . For the infinite line there are two  $\phi_\omega$  solutions for each  $\omega$ , which allow a decomposition of wave packets arriving simultaneously from both  $-\infty$  and  $+\infty$ . On the other hand, for the semi-infinite line the boundary condition selects a single  $\phi_\omega$  solution for each  $\omega$ . This still allows for a decomposition of a wave packet, which this time can arrive only from  $+\infty$ . The situation for Reissner-Nordström is similar to the infinite line, while negative-mass Schwarzschild is similar to the semi-infinite line (we consider the  $r < 0$  side of the Schwarzschild singularity since there  $t$  is time-like and one can consider scattering experiments).

Thus we naturally define the time evolution for negative-mass Schwarzschild by decomposing the initial conditions (defined only at  $r = -\infty$ ) into the regular eigen-functions  $\phi_{1\omega}$  alone and then proceeding as usual to define the time evolution. Since  $\phi_{1\omega}$  is smooth at  $r = 0$ , the time evolution will be smooth there too. As it turns out it was found already in [8] by somewhat formal arguments that there exists a unique time evolution for negative-mass Schwarzschild, which is probably the same as the one we just explicitly described. For RN on the other hand we differ as we get wave-regularity after considering both sides of the singularity, while they do not.

#### *Perspectives on the boundary conditions for Schwarzschild*

In the Schwarzschild case we simply impose the boundary condition that the scalar field be regular at  $r = 0$ . This does not conform with either the Dirichlet or Neumann b.c.; namely, neither  $\phi$  nor its radial derivative vanishes at  $r = 0$ . In fact, the Dirichlet or Neumann b.c. are both inconsistent with the asymptotic behavior near the singularity (due to the presence of a divergent mode).

Yet, there is a physically appealing procedure to obtain our regularity b.c. from the Dirichlet or Neumann b.c. (or a mixture). We can cutoff space at some  $r_1 < 0$  close to the singularity, and then take the limit  $r_1 \rightarrow 0$ . Since all modes are well-behaved at  $r = r_1$ , we are free to impose either Dirichlet or Neumann b.c. there. Let us denote as before the solution regular at  $r = 0$  by  $\phi_{1\omega}$ , and some other independent and necessarily singular solution by  $\phi_{2\omega}$ . We are looking for a linear combination of the two,  $\phi_\omega = a\phi_{1\omega} + b\phi_{2\omega}$ , that will satisfy the boundary conditions at  $r_1$ . If we impose Dirichlet we need

$$0 = \phi_\omega(r_1) = a\phi_{1\omega}(r_1) + b\phi_{2\omega}(r_1) . \quad (3.10)$$

As we take  $r_1 \rightarrow 0$   $\phi_{1\omega}$  remains finite while  $\phi_{2\omega}$  diverges with a log singularity, and hence we must take  $b = 0$ , namely the “regular solution b.c.”

If we choose Neumann conditions instead, we note that again while  $\phi'_{1\omega}$  remains finite  $\phi'_{2\omega}$  diverges with a  $1/r$  singularity and hence we are again forced to take  $b = 0$ . Altogether we find that in both cases as  $r_1 \rightarrow 0$  we are left with a unique b.c., namely our “regular b.c.”

### 3.3 Normal form of the radial equation

Transforming to a new radial coordinate (the so called “tortoise coordinate”)  $r^*(r)$  defined by

$$dr^* = \frac{dr}{f(r)}, \quad (3.11)$$

and to a new field variable

$$\phi^* := r\phi \quad (3.12)$$

(and correspondingly  $\phi_\omega^* := r\phi_\omega$ ), the wave equation (3.2) and the radial equation (3.5) take the standard forms

$$f^{-1} [\partial_{tt} - \partial_{r^*r^*} + V_{\text{eff}}(r^*)] \phi^* = 0 \quad (3.13)$$

and

$$[-\partial_{r^*r^*} + V_{\text{eff}}(r^*) - \omega^2] \phi_\omega^* = 0. \quad (3.14)$$

Here the effective potential  $V_{\text{eff}}$  is given by  $V_{\text{eff}}^{\text{geodesic}}$ , the effective potential for particles, with the substitutions  $l^2 \rightarrow l(l+1)$  and  $E \rightarrow 0$ ,<sup>10</sup> plus an extra term  $\Delta V_{\text{eff}}$ :

$$V_{\text{eff}}(r^*) = \Delta V_{\text{eff}} + f \frac{l(l+1)}{r^2}, \quad (3.15)$$

where

$$\Delta V_{\text{eff}}(r^*) = \frac{f}{r} \partial_r f. \quad (3.16)$$

We find it instructive to explore the leading terms in the radial equation at  $r = 0$ , when this equation is expressed in terms of  $r^*$  rather than  $r$ .

We start by looking at the Reissner-Nordström case. To leading order near  $r \sim 0$

$$r^* \cong \frac{r^3}{3Q^2}, \quad (3.17)$$

and hence

$$V_{\text{eff}} \cong -2 \frac{Q^4}{r^6} \cong -\frac{2}{9r^{*2}}. \quad (3.18)$$

Thus even though the wave equation in the form (3.5) is smooth, the effective potential in the normal form is unbounded from below; hence we will study later (in section 4) its response to high-frequency waves, where all features of the potential other than its leading term  $\propto r^{*-2}$  are irrelevant. Note that such potentials of the type  $V = -c/r^{*\alpha}$  are special (see for instance [28]). Considering a larger class of potentials  $V = -c/r^{*\alpha}$  with  $c, \alpha > 0$ ,

---

<sup>10</sup>in principle  $E$  is to be now replaced by  $\omega$ , but the latter already appears explicitly in Eq. (3.14). Recall also that we assume at this stage a neutral massless scalar field, hence  $m = q = 0$ .

then  $\alpha = 2$  is a critical value describing a conformal quantum mechanics <sup>11</sup>, namely  $c$  is dimensionless. For  $0 < \alpha < 2$  the spectrum is bounded from below even though the classical potential is not, while for  $\alpha > 2$  the spectrum is not bounded from below. For the critical value  $\alpha = 2$  there is a critical value for  $c$ ,  $c = 1/4$ . For  $c < 1/4$  the potential is still mild enough to have a spectrum bounded from below (actually at zero), while for  $c > 1/4$  it is not. So the numerical coefficient  $c = 2/9$  in (3.18) is important. We will see later (in section 5) that  $c$  varies over our examples (it depends on the number of dimensions, but always  $c < 1/4$  in the charged case), and that it determines the high-energy transmission properties of the singularity.

At  $r^* = 0$  the radial equation (3.14) has a regular singularity, and we may look for the characteristic exponents  $\rho$  defined by  $\phi_\omega^* \cong r^{*\rho}$ . These satisfy the characteristic equation

$$\rho(\rho - 1) + \frac{2}{9} = 0,$$

leading to the two roots

$$\rho_{1,2} = \frac{1}{3}, \frac{2}{3}, \quad (3.19)$$

which are independent of  $\omega$ . Translating back from  $r^*$  to  $r$  using the transformation (3.12,3.17) we get the exponents  $r^0$  and  $r^1$ , exactly as expected for a smooth second-order equation.

For Schwarzschild one may repeat the calculations based on the leading behavior of  $f_{\text{Schw}}$  (2.3) and find

$$r^* \cong -\frac{r^2}{4M}, \quad (3.20)$$

leading to

$$V_{\text{eff}} \cong -4\frac{M^2}{r^4} \cong -\frac{1}{4r^{*2}}. \quad (3.21)$$

Thus we have here the critical value  $c = 1/4$  (independent of the spacetime dimension, see section 5).

Attempting  $\phi_\omega^* \cong r^{*\rho}$  one obtains the characteristic equation

$$\rho(\rho - 1) + \frac{1}{4} = 0,$$

which yields

$$\rho_1 = \rho_2 = \frac{1}{2}. \quad (3.22)$$

The equality of the two exponents implies the presence of a log term in one of these solutions. Again translating back the characteristic exponents to the  $r$  coordinate we get the  $r^0$ ,  $\log(r)$  behavior which was derived above from Eq. (3.9).

---

<sup>11</sup>if we replace  $\omega^2 \rightarrow \omega$  in (3.14).

### 3.4 Characteristic formulation

Having defined the ‘‘tortoise’’ coordinate  $r^*$  (3.11) and the effective potential (3.15) we can now return to spell out in detail the definition of time evolution in the characteristic formulation.

The coordinate  $r^*$  approaches  $-\infty$  as  $r \rightarrow -\infty$  and  $+\infty$  as  $r \rightarrow r_-$ . Notice that the effective potential decays as  $r^{-2} \simeq r^{*-2}$  at large negative  $r$ , and as  $f \propto r - r_-$  (which is exponentially small in  $r^*$ ) at the inner horizon. Therefore, in each of these asymptotic boundaries the radial function is a superposition of the two asymptotic solutions

$$\phi_\omega^* \cong \exp(+i\omega r^*) \text{ and } \phi_\omega^* \cong \exp(-i\omega r^*) . \quad (3.23)$$

Defining the Eddington-like coordinates

$$v := t - r^* , \quad u := t + r^* ,$$

the above two asymptotic solutions at both edges  $r^* \rightarrow \pm\infty$  read, for a particular  $\omega$  component of  $\phi^*$ ,

$$\phi^* \cong \exp(i\omega u) \text{ and } \phi^* \cong \exp(i\omega v) ,$$

respectively. The non-decomposed field at both asymptotic edges takes the form

$$\phi^*(r^* \rightarrow \pm\infty) \cong f_\pm(v) + g_\pm(u),$$

where  $f_\pm(v)$  and  $g_\pm(u)$  are arbitrary functions (the ‘‘ $\pm$ ’’ stands for the two asymptotic regions  $r^* \rightarrow \pm\infty$ , i.e. to the inner horizon and to large negative  $r$ ). In the characteristic initial-value formulation one needs to specify the ingoing component  $f_-(v)$  at  $\mathcal{I}^-$  and the component  $g_+(u)$  coming from the inner horizon. These two functions should uniquely determine the time evolution in the relevant piece of spacetime. This evolution is defined as follows. First, Fourier-decompose these two initial functions:

$$f_-(v) = \int f_v(\omega_v) \exp(i\omega_v v) d\omega_v ,$$

$$g_+(u) = \int g_u(\omega_u) \exp(i\omega_u u) d\omega_u .$$

Next, we define a set of basis solutions  $\phi_{(\omega_v,0)}^*(r^*, t)$  and  $\phi_{(0,\omega_u)}^*(r^*, t)$  (for each  $\omega_v$  and  $\omega_u$ ) as follows:  $\phi_{(\omega_v,0)}^*$  is the solution evolving from the characteristic initial conditions

$$f_-(v) = \exp(i\omega_v v) , \quad g_+(u) = 0 .$$

Similarly,  $\phi_{(0,\omega_u)}^*$  is the solution evolving from the characteristic initial conditions

$$f_-(v) = 0 , \quad g_+(u) = \exp(i\omega_u u) .$$

The two functions  $\phi_{(\omega_v,0)}^*$  and  $\phi_{(0,\omega_u)}^*$  are constructed from the radial functions  $\phi_\omega^*(r^*)$  (with  $\omega = \omega_v$  and  $\omega = \omega_u$ , respectively); see appendix C for details.

Once  $\phi_{(\omega_v,0)}^*$  and  $\phi_{(0,\omega_u)}^*$  are defined, the time evolution of the field  $\phi^*$  emerging from the characteristic initial data  $f_-(v)$  and  $g_+(u)$  is simply given by

$$\begin{aligned} \phi^*(r^*, t) &= \int f_v(\omega_v) \phi_{(\omega_v,0)}^*(r^*, t) d\omega_v \\ &\quad + \int g_u(\omega_u) \phi_{(0,\omega_u)}^*(r^*, t) d\omega_u. \end{aligned}$$

We conclude that the unique extension of the radial functions  $\phi_\omega^*(r^*)$  across the  $r = 0$  singularity naturally leads to a unique time evolution for any set of characteristic initial functions  $f_-(v)$  and  $g_+(u)$ .

#### 4. Transmission cross section in Reissner-Nordström

Having demonstrated a resolution of the  $r = 0$  singularity we turn in this section to examine its nature through scattering. Here we shall only consider the charged (Reissner-Nordström) case. Full reflection from the negative-mass Schwarzschild singularity will be considered together with the  $d > 4$  cases at the end of subsection 5.1. We focus here on the transmission of high-frequency incoming waves through the  $r = 0$  singularity (from now on we will use “high-energy” to mean “high-frequency” by a slight abuse of language originating from the quantum theory).

We first study the effective potential  $V_{\text{eff}}$ , and especially its asymptotic form at small  $r$ . Then we compute the transmission and reflection coefficients for fixed  $l$  in the high-energy limit. Finally we combine that result with the high- $l$  limit, where the partial cross section vanishes. We sum over  $l$  and obtain the  $\omega$  dependence of the (high-energy) total cross section for transmission.

##### 4.1 General features of the effective potential

Consider first the qualitative behavior of the effective potential  $V_{\text{eff}}$ . For concreteness we shall consider here a wave propagating from past null infinity of the negative- $r$  universe towards  $r = 0$ . At large  $|r|$ , we have the usual centrifugal barrier

$$V_{\text{eff}} \cong \frac{l(l+1)}{r^2} \quad (|r| \gg M). \quad (4.1)$$

At small  $|r|$ , the potential takes the asymptotic form

$$V_{\text{eff}} \cong l(l+1) \frac{Q^2}{r^4} - 2 \frac{Q^4}{r^6} \quad (|r| \ll Q). \quad (4.2)$$

Here we only keep the leading order in  $r/Q$ . We do keep, however, the term  $\propto r^{-4}$  in the right-hand side because it is proportional to  $l(l+1)$ . This term will become important for partial waves of sufficiently large  $l$ , which are involved in the calculation of the total high-energy transmission cross-section (see below).

The contribution of any particular  $l$  to the total high-energy cross-section is suppressed by the kinematic factor  $k^{-2}$  in Eq. (4.14) below (while it will turn out that  $\sigma \gg k^{-2}$ ).

Therefore, at high energy the total cross section is dominated by partial waves with  $l \gg 1$ , which we shall assume hereafter. Such waves of relatively small or moderate energy will be reflected already at the large- $|r|$  centrifugal barrier (4.1). Only waves with sufficiently high energy,  $\omega > l/Q$ , will penetrate into the central region  $|r| \ll Q$ . The scattering features of these high-energy waves will be dominated by the small- $|r|$  potential (4.2). This potential has a peak value (hereafter we often replace  $l(l+1)$  by  $l^2$ , which is justified because  $l \gg 1$ )

$$V_{\max} \cong \frac{l^6}{27Q^2},$$

located at

$$|r| \cong r_{peak} := \sqrt{3}Q/l.$$

It acts as a repulsive barrier ( $\propto r^{-4}$ ) at  $Q \gg |r| > r_{peak}$ , and as a potential well ( $\propto -r^{-6}$ ) at  $|r| < r_{peak}$ .

The above discussion immediately suggests that partial waves with  $\omega \ll \omega_{peak}$ , where

$$\omega_{peak} := \sqrt{V_{\max}} \cong \frac{l^3}{\sqrt{27}Q}, \quad (4.3)$$

will be fully reflected by the potential barrier at  $|r| > r_{peak}$ . However, partial waves with  $\omega \gg \omega_{peak}$  will predominantly feel the potential well  $\propto -r^{-6}$  at  $|r| < r_{peak}$ . These waves will be partially transmitted, as we analyze in the next subsection.

For later convenience we transform the small- $|r|$  potential from  $r$  to  $r^*$ , using  $r^3 \cong 3Q^2 r^*$ :

$$V_{\text{eff}} \cong \frac{l^2}{Q^{2/3}(3r^*)^{4/3}} - \frac{2}{9r^{*2}} \quad (r \ll Q). \quad (4.4)$$

The peak is located at

$$|r^*| \cong r_{peak}^* := \sqrt{3}Q/l^3.$$

Although we are primarily considering here a wave coming from the negative- $r$  past null infinity, the case of a wave propagating from  $r_-$  towards  $r = 0$  may be treated in exactly the same manner. Note that the small- $|r|$  potential (4.2) or (4.4) is even in  $r$  or  $r^*$ , respectively. Consequently the high-energy transmission amplitude for partial waves is the same for both cases. (Obviously the transmission probability is exactly the same, even for finite  $\omega$ .)

## 4.2 Amplitudes at high energy and fixed $l$

It is instructive to look at the scattering in the high-energy limit. Normally, the potential is bounded, hence the transmission amplitude approaches 1 and the reflection vanishes at this limit. However, here we have an unbounded (attractive) potential near  $r = r^* = 0$ , which leads to partial reflection even at the high-energy limit.

For fixed  $l$  and high energy,  $\omega \gg \omega_{peak}$ , the potential is dominated by

$$V_{\text{eff}} \cong -\frac{2}{9r^{*2}} \equiv V_{\text{eff,sing}}.$$

We therefore need to solve the scattering problem

$$0 = [-\partial_{r^*r^*} + V_{\text{eff,sing}}(r^*) - \omega^2]\phi^*. \quad (4.5)$$

Passing to the dimensionless variable <sup>12</sup>

$$x = -r^* \omega, \quad (4.6)$$

the equation is transformed into

$$0 = [-\partial_{xx} - \frac{2}{9x^2} - 1] \phi^*. \quad (4.7)$$

Its general solution is

$$\phi^* = c_1 \phi_1^* + c_2 \phi_2^*, \quad (4.8)$$

with

$$\begin{aligned} \phi_1^* &= \sqrt{x} J_{1/6}(x), \\ \phi_2^* &= \sqrt{x} J_{-1/6}(x) \end{aligned} \quad (4.9)$$

(for  $x > 0$ ), where  $J_n$  are Bessel functions of order  $n$  (see appendix D). The coefficients  $c_1, c_2$  will be determined below.

In order to extend the solution (4.8) across  $x = 0$ , we first express it in terms of  $r$ . Recall that at small  $r$ ,

$$r^* \cong \frac{r^3}{3Q^2},$$

and, furthermore,  $r^*(r)$  is analytic at  $r = 0$ . From the local behavior of the Bessel functions  $J_n(\lambda)$  near  $\lambda = 0$  (see appendix D), and that of  $r^*$  near  $r = 0$ , it follows that  $\phi_1^*$  and  $\phi_2^*$  take the form

$$\begin{aligned} \phi_1^* &= r^2 A_{1/6}^J(r^6), \\ \phi_2^* &= r A_{-1/6}^J(r^6), \end{aligned} \quad (4.10)$$

where  $A_{\pm 1/6}^J(\lambda)$  are some real functions (for real  $\lambda$ ), analytic at  $\lambda = 0$ . Obviously both  $\phi_1^*(r)$  and  $\phi_2^*(r)$  have a unique real analytic extension through  $r = 0$ .<sup>13</sup> The form of Eq. (4.10) ensures that  $\phi_1^*$  extends as an even function, and  $\phi_2^*$  as an odd one. Hence for negative  $x$  we get

$$\begin{aligned} \phi_1^*(x) &= \sqrt{|x|} J_{1/6}(|x|), \\ \phi_2^*(x) &= -\sqrt{|x|} J_{-1/6}(|x|). \end{aligned} \quad (4.11)$$

In order to get the coefficients  $c_1, c_2$  – and the transmission and reflection coefficients – we impose the large- $r^*$  boundary conditions. Since we are considering here a wave propagating from (say) past null infinity (large negative  $r^*$ ), we assume that no waves are entering from the inner horizon ( $r^* \rightarrow +\infty$ ). This corresponds to pure asymptotic behavior

---

<sup>12</sup>The negative sign in the definition of  $x$  was introduced in order for the incoming wave to propagate from large positive  $x$  values (null infinity) towards smaller  $x$  values.

<sup>13</sup>Recall that  $\phi_1^*(r)$  and  $\phi_2^*(r)$  must extend to  $r > 0$  as real and analytic functions, because the radial equation (3.5) is real and analytic (and  $\phi_1^*, \phi_2^*$  are real at  $r < 0$ ).



$\propto \exp(-i\omega r^*) = \exp(ix)$  at  $x \rightarrow -\infty$ . Thus, in terms of  $x$  the asymptotic behavior at the boundaries is

$$\begin{aligned}\phi^* &\cong \exp(ix) + R(\omega) \exp(-ix) && \text{at } x \rightarrow +\infty, \\ \phi^* &\cong T(\omega) \exp(ix) && \text{at } x \rightarrow -\infty.\end{aligned}\tag{4.12}$$

Note that since  $\omega$  got scaled out of the equation  $T(\omega)$ ,  $R(\omega)$  are actually independent of  $\omega$ .

The asymptotic form of the Bessel functions for large (positive) argument is given in Eq. (D.4). For  $n = 1/6$  it reads

$$\exp(\pm i|x|) \cong \sqrt{\pi|x|/2} \exp(\pm i\pi/3) \left[ (1 \pm i\sqrt{3})J_{1/6}(|x|) \mp 2iJ_{-1/6}(|x|) \right].$$

Applying it first to the inner-horizon boundary ( $x \rightarrow -\infty$ ), along with Eq. (4.11), one finds

$$\begin{aligned}c_1 &= \sqrt{\pi/2} \exp(-i\pi/3) (1 - i\sqrt{3}) T(\omega), \\ c_2 &= -i\sqrt{2\pi} \exp(-i\pi/3) T(\omega).\end{aligned}$$

Similarly, when applied to the null-infinity boundary ( $x \rightarrow +\infty$ ), along with Eq. (4.9), it yields

$$\begin{aligned}c_1 &= \sqrt{\pi/2} \left[ \exp(i\pi/3) (1 + i\sqrt{3}) + \exp(-i\pi/3) (1 - i\sqrt{3}) R(\omega) \right], \\ c_2 &= -i\sqrt{2\pi} \left[ \exp(i\pi/3) - \exp(-i\pi/3) R(\omega) \right].\end{aligned}$$

Combining the two expressions for  $c_1, c_2$  and solving for  $R$  and  $T$ , one obtains

$$R = \frac{\sqrt{3}}{2}i, \quad T = \frac{1}{2}.\tag{4.13}$$

We conclude that for any  $l$ , at the high-energy limit a fraction  $|R|^2 = 3/4$  of the influx is reflected and a fraction  $|T|^2 = 1/4$  is transmitted to the other side of the  $r = 0$  singularity. As was mentioned above, this applies to both waves coming from past null infinity (of the negative- $r$  universe beyond the singularity) and waves coming from the inner horizon towards the  $r = 0$  singularity.

### 4.3 Summing over $l$

The total cross section for transmission is given by a sum over all partial waves  $l$ :

$$\sigma = \frac{\pi}{k^2} \sum_{l=0}^{\infty} (2l+1) |T_l|^2,\tag{4.14}$$

where  $k$  is the momentum of the incoming plane wave ( $k = \omega$  for a massless field, which we assume from now on in this subsection). We shall consider here the cross section at the high-energy limit. As mentioned above, at this limit the total cross section is dominated by the contribution from modes  $l \gg 1$ , because each particular  $l$  is suppressed by the

factor  $\omega^{-2}$ , while it will turn out that  $\sigma \gg \omega^{-2}$ . The result of the previous subsection,  $|T_l|^2 \cong 1/4$ , holds for  $l$  values that are not too large. However, for any fixed and large  $\omega$  there is some large enough  $l$  where the transmission practically vanishes. For instance, for classical flat-space scattering off a rigid target of length scale  $L$  (“rigid” means here  $\omega$ -independent  $L$ ), if the impact parameter  $b$  is much larger than  $L$  then the absorption vanishes. Since  $b = l/p$  (and  $p = \omega$  in our massless case) we see that for  $l > L\omega$  the absorption vanishes. We will now show that in our case the suppression of transmission already happens for  $l > (Q\omega)^{1/3}$ .

A rough estimate of the total large- $\omega$  cross section can be easily done based on the qualitative features of  $V_{\text{eff}}$  at small  $r$ . For  $\omega \gg \omega_{\text{peak}}$ , where  $\omega_{\text{peak}}$  is defined in (4.3), the above high-energy result  $|T_l|^2 \cong 1/4$  holds. For  $\omega$  significantly smaller than  $\omega_{\text{peak}}$  the incoming wave will encounter the potential barrier

$$V_{\text{eff}} \cong \frac{l^2}{Q^{2/3}(3r^*)^{4/3}} \quad (4.15)$$

and will be tunnelling suppressed there. [In fact, an effective tunnelling suppression requires that  $\omega\Delta$  is greater than 1, where  $\Delta$  is the tunnelling length scale in the barrier in terms of  $r^*$ , i.e. from (4.15)  $\Delta \sim (\omega^3 Q/l^3)^{-1/2}$ . But this is automatically satisfied because  $\omega\Delta \sim (\omega Q/l^3)^{-1/2}$  is roughly  $(\omega_{\text{peak}}/\omega)^{1/2}$ , which is  $\gg 1$  in the present discussion.] Thus, for a rough estimate of the large- $\omega$  cross section we may substitute  $|T_l|^2 \cong 1/4$  for  $l \ll l_c$  and negligible  $|T_l|^2$  for  $l \gg l_c$ , where

$$l_c := \sqrt{3}(Q\omega)^{1/3} \quad (4.16)$$

can be read off the expression for  $\omega_{\text{peak}}$  (4.3).

Equation (4.14) then yields the total cross section:

$$\sigma \sim \frac{l_c^2}{\omega^2} \sim \frac{Q^{2/3}}{\omega^{4/3}}. \quad (4.17)$$

The total cross section may also be obtained from  $l_c$  by a simple argument: the critical maximal impact parameter for transmission is  $b_{\text{max}} = l_c/\omega$ , and hence the total size (cross-section) of the target for transmission is

$$\sigma \sim b_{\text{max}}^2 = \frac{l_c^2}{\omega^2} \sim \frac{Q^{2/3}}{\omega^{4/3}}. \quad (4.18)$$

In the above estimate we have not taken into account the contribution coming from the range  $l \sim l_c$ . A more rigorous derivation of the cross section (4.17,4.18), which properly treats this range as well, may be done by analyzing the rescaling properties of the small- $r$  scattering problem, i.e.

$$[-\partial_{r^* r^*} + V_{\text{eff}} - \omega^2]\phi = 0 \quad (4.19)$$

with the potential (4.4). Transforming to a new dimensionless variable

$$x := -\frac{l^3}{Q}r^*, \quad (4.20)$$

the equation becomes

$$[-\partial_{xx} + \hat{V}(x) - \Omega^2]\phi = 0,$$

where

$$\hat{V}(x) = -\frac{2}{9x^2} + \frac{1}{(3x)^{4/3}}$$

and

$$\Omega := \frac{Q}{l^3}\omega.$$

The boundary conditions at large  $|x|$  are, in accordance with Eq. (4.12),

$$\begin{aligned} \phi^* &\cong \exp(i\Omega x) + R(\Omega) \exp(-i\Omega x) & \text{at } x \rightarrow +\infty, \\ \phi^* &\cong T(\Omega) \exp(i\Omega x) & \text{at } x \rightarrow -\infty. \end{aligned} \quad (4.21)$$

Hence in this limit of large  $\omega$  and large  $l$  the transmission amplitude depends only on  $\Omega$ , i.e.

$$T = T\left(\frac{\omega Q}{l^3}\right). \quad (4.22)$$

The cross section is

$$\sigma = \frac{\pi}{\omega^2} \sum_{l=0}^{\infty} (2l+1) |T_l|^2 \cong \frac{2\pi}{\omega^2} \int l \left|T\left(\frac{\omega Q}{l^3}\right)\right|^2 dl,$$

where we used  $l \gg 1$  to replace  $2l+1$  by  $2l$  and the sum by an integral. Finally, transforming from  $l$  to  $\hat{l} := l/(\omega Q)^{1/3}$  we find

$$\sigma \cong c \frac{Q^{2/3}}{\omega^{4/3}}, \quad (4.23)$$

where

$$c = 2\pi \int \hat{l} |T(\hat{l}^{-3})|^2 d\hat{l},$$

in agreement with the above estimate (4.17).

Having found the total cross section for transmission, one may inquire about the total cross section for scattering. At large distances this is just like a Coulomb problem with a length scale  $M$ . Due to the infinite range of the gravitational force, we expect the cross section for scattering to be infinite for a massive field. However, for a massless field the scattering potential decays (after subtracting the standard centrifugal piece  $l(l+1)/r^{*2}$ ) as  $\ln(r^*/M)/r^{*3}$ . This is a short-range potential, hence we expect a finite scattering cross-section in the massless case.

The peculiar  $\omega$  dependence of the transmission cross section (4.17) through the singularity can be compared with two other systems. For black holes with non-zero area the large  $\omega$  absorption cross section through the event horizon tends to the geodesic cross section, and hence  $\sigma \sim \omega^0$ . For elementary particles, on the other hand, the high-energy scattering cross section  $\sigma_{\text{scat}} \sim \omega^{-2}$  which is the kinematical factor which multiplies the dimensionless scattering amplitude. So we see that this system lies between the two examples above.

Another interpretation issue is whether the partial transmission/partial scattering behavior at large  $\omega$  should be interpreted as a beam splitter for single particles. The question

is whether a wave packet can be made small enough so that it fits into a target of size  $\sim \omega^{-2/3}$  – otherwise it will not be fully split. Imagine that we set a “lens” (one which affects  $\phi$  waves) at a distance  $f \sim \omega^0 \gg Q$  from the black hole. We know that the spot size at focus can be made as small as  $\lambda f/D$ , where  $\lambda = 2\pi/\omega$  is the wavelength and  $D$  is the aperture size, and we here imagine that space is flat and we need to hit a target with the same cross section as the  $r = 0$  singularity. From  $\lambda f/D \ll \omega^{-2/3}$  we find that we need  $D \geq \omega^{-1/3}$ . So such focusing can be readily achieved, even with a small size lens. This suggest that the singularity may indeed act as a beam splitter. Note, however, that in the above analysis we only considered incoming *plane waves* (or pure partial waves with well-defined  $l$  values). In order to verify the beam-splitter behavior one needs to explicitly analyze the transmission amplitude in the geometrical configuration considered above (i.e. a narrow beam focused on a small region near  $r = 0$ ). This calculation is beyond the scope of the present paper.

## 5. Generalizing the backgrounds

### 5.1 Higher dimensions

The background RN metric and gauge field in  $d \geq 4$  dimensions are [29]

$$\begin{aligned} ds^2 &= -f dt^2 + f^{-1} dr^2 + r^2 d\Omega_{d-2}^2 \\ A &= -\frac{Q}{r^{d-3}} dt \\ f &= 1 - \frac{r_+^{d-3} + r_-^{d-3}}{r^{d-3}} + \frac{(r_+ r_-)^{d-3}}{r^{2(d-3)}} \end{aligned} \quad (5.1)$$

The mass and charge are

$$\begin{aligned} M &= \frac{(d-2)\Omega_{d-2}}{16\pi} (r_+^{d-3} + r_-^{d-3}) \\ Q &= \text{const} \sqrt{r_+ r_-}^{d-3} \end{aligned} \quad (5.2)$$

where  $\Omega_{d-2}$  is the area of the  $d-2$  sphere, and we do not fix the constant in front of the charge which depends on the normalization chosen for the vector field. In order to get  $d$ -dimensional Schwarzschild one sets  $r_- = 0$ ,  $r_+ = r_0$ .

After separation of the time variable ( $\partial_{tt} \rightarrow -\omega^2$ ) the scalar wave equation becomes

$$\left[ \frac{1}{f r^{d-2}} \partial_r f r^{d-2} \partial_r - \frac{l(l+d-3)}{f r^2} + f^{-2} \omega^2 \right] \phi_\omega = 0. \quad (5.3)$$

Considering the charged case first, and comparing with the 4d case (3.6) one notes a change: the equation (5.3) is not regular anymore at  $r = 0$  (since  $f r^{d-2}$  has a pole). Actually it is regular-singular with leading behavior

$$\left[ -\partial_{rr} + \frac{d-4}{r} \left( 1 + O(r^{d-3}) \right) \partial_r + l(l+d-3) O(r^{2(d-4)}) + \omega^2 O(r^{4(d-3)}) \right] \phi_\omega = 0. \quad (5.4)$$

The two solutions of the characteristic equation are  $r^0, r^{d-3}$ . Since the difference of the exponents is integral it is possible *a priori* that the  $r^0$  solution has a log piece of the following form  $\phi_\omega = r^0 + \dots + \log(r) r^{d-3} + \dots$ , however it is seen not to be the case by explicitly Taylor expanding  $\phi_\omega$  in the differential equation (5.4).

For Schwarzschild, on the other hand, one finds the same leading behavior as in 4d

$$\left[ \partial_{rr} + \frac{1}{r} \partial_r + \dots \right] \phi_\omega = 0 \quad (5.5)$$

and thus the leading behavior of the two independent solutions is still  $r^0, \log(r)$ .

As in subsection 3.3 we may find the normal form of the radial equation (5.3). The  $r^*$  coordinate is defined by

$$dr^* = \frac{dr}{f} \quad , \quad (5.6)$$

the field is redefined by

$$\phi^* := r^{(d-2)/2} \phi \quad , \quad (5.7)$$

and the resulting effective potential is

$$\begin{aligned} V_{\text{eff}} &= \Delta V_{\text{eff}} + f \frac{l(l+d-3)}{r^2} \\ \Delta V_{\text{eff}} &= \frac{d-2}{2} \frac{f}{r^{(d-2)/2}} \partial_r (r^{(d-4)/2} f) \end{aligned} \quad (5.8)$$

where we use the same notations as in subsection 3.3.

We start by looking at the charged case. The leading behavior near the singularity (at  $r = 0$ ) is

$$\begin{aligned} r^* &\cong \frac{r^{2d-5}}{(2d-5)(r_+ r_-)^{(d-3)}} \\ V_{\text{eff}} &\cong -\frac{(d-2)(3d-8)}{4(2d-5)^2} \frac{1}{r^{*2}} \end{aligned} \quad (5.9)$$

Given an effective potential  $V_{\text{eff}} \simeq -c/r^{*2}$  the order  $n$  of the Bessel functions which appear in the high  $\omega$  solution is given by (see appendix D)

$$n^2 = \frac{1}{4} - c \quad . \quad (5.10)$$

Hence, the second equation in (5.9) determines

$$|n|_{\text{RN}} = \frac{1}{4} \frac{d-3}{d-5/2} \quad (5.11)$$

generalizing the 4d result  $|n| = 1/6$  (4.9).

We note in passing that for the 2d black hole we will show in the next subsection that  $V_{\text{eff}} \simeq -3/(16r^{*2})$  and hence one can define an “effective” or “equivalent” RN dimension to be  $d_{\text{eff}} = \infty$  or  $11/4$ , and  $|n|_{2d} = 1/4$ .

The transmission and reflection coefficients for high  $\omega$  and fixed  $l$  follow from the asymptotics of the Bessel functions as in subsection 4.2:

$$\begin{aligned} |R| &= |\cos(n\pi)| \\ |T| &= |\sin(n\pi)| \end{aligned} \tag{5.12}$$

The  $\omega$  dependence of the total cross section for transmission can be derived along the lines of subsection 4.3. The leading terms in the potential (5.8) at  $r \sim 0$  are

$$V_{\text{eff}} \simeq l^2 \frac{(r_+ r_-)^{d-3}}{r^{2d-4}} - \frac{d-2}{2} \left(\frac{3}{2}d-4\right) \frac{(r_+ r_-)^{2(d-3)}}{r^{4d-10}} . \tag{5.13}$$

For fixed  $l$  the potential has a maximum at

$$r_{\text{peak}} \simeq \frac{1}{\sqrt[d-3]{l}} . \tag{5.14}$$

Equating  $V(r_{\text{peak}})$  with  $\omega^2$  we get the transition value for  $l$ :

$$l_c \sim \omega^{\frac{d-3}{2d-5}} . \tag{5.15}$$

Finally, we evaluate the total transmission cross section by employing qualitative classical-mechanics considerations. Classically the cross section is obtained by estimating the maximal value of impact parameter  $b$  for which a significant transmission (or scattering, in the more general context) still occurs. Using  $b = l/\omega$  we get  $b_{\text{max}} \sim l_c/\omega$ . Since in  $d$  dimensions the cross section scales as  $b_{\text{max}}^{d-2}$ , we find

$$\sigma \sim b_{\text{max}}^{d-2} \sim \left(\frac{l_c}{\omega}\right)^{d-2} \sim \omega^{-\frac{(d-2)^2}{2d-5}} . \tag{5.16}$$

For Schwarzschild black holes the leading behavior near the singularity (at  $r = 0$ ) is

$$\begin{aligned} r^* &\cong -\frac{r^{d-2}}{(d-2)r_0^{d-3}} \\ V_{\text{eff}} &\cong -\frac{1}{4r^{*2}} . \end{aligned} \tag{5.17}$$

Thus independently of dimension one has  $c = 1/4$  and hence total reflection:

$$\begin{aligned} n &= 0 \\ T &= 0 . \end{aligned} \tag{5.18}$$

## 5.2 The 2d black hole

Black holes in two dimensions are apparently outside the pattern of the  $d \geq 4$  black holes discussed in the previous sections (although as we shall recall [4] they turn out to share similar features). Such solutions require, for instance, the presence of a dilaton. In this

subsection we shall consider two dimensional dilaton gravity with an Abelian gauge field which is inspired by string theory. The action is <sup>14</sup>

$$S = \int d^2x \sqrt{-g} e^{-2\Phi} \left( R + 4g^{\mu\nu} \partial_\mu \Phi \partial_\nu \Phi - \frac{1}{4} F^2 - \lambda \right), \quad (5.19)$$

where  $g_{\mu\nu}$  is the (string frame) metric,  $\mu, \nu = 0, 1$ ,  $\Phi$  is the dilaton,  $F_{\mu\nu}$  is the field strength of an Abelian gauge field  $A_\mu$ , and  $\lambda$  is the cosmological constant. In this two dimensional theory, the charged black hole solution is given by [30]

$$\begin{aligned} ds^2 &\propto f^{-1} d\rho^2 - f dt^2 \\ A &\propto -\frac{Q}{r} dt \\ \Phi(\rho) &= \Phi_0 - \frac{1}{2}\rho, \end{aligned} \quad (5.20)$$

where  $\Phi_0$  is a constant and

$$f(r) = 1 - \frac{2M}{r} + \frac{Q^2}{r^2}, \quad r = e^\rho. \quad (5.21)$$

Note that here  $ds^2 \propto f^{-1} \frac{dr^2}{r^2} - f dt^2$ , which is different from the generic  $d \geq 4$  cases in eq. (5.1). Nevertheless, the geometry of this 2d black-hole is similar to a two dimensional slice of the Reissner-Nordström solution, whose complete Penrose diagram is given in figure 2. In the 4d case every point in figure 2 is actually a two sphere, while in the 2d case there is a non-trivial dilaton instead.

An uncharged scalar field is minimally coupled to the background above as follows:

$$S = \int d^2x \sqrt{-g} e^{-2\Phi} \left( R + 4g^{\mu\nu} \partial_\mu \Phi \partial_\nu \Phi - \frac{1}{4} F^2 - \lambda - g^{\mu\nu} \partial_\mu \psi \partial_\nu \psi - m^2 \psi^2 \right), \quad (5.22)$$

where in this section  $\psi$  denotes the scalar field to distinguish it from the dilaton  $\Phi$ . The wave equation of  $\psi$  is:

$$\square_\Phi \psi = \frac{e^{2\Phi}}{\sqrt{-g}} \partial_\mu \sqrt{-g} e^{-2\Phi} g^{\mu\nu} \partial_\nu \psi = (\partial_r r^2 f \partial_r - f^{-1} \partial_{tt}) \psi = m^2 \psi, \quad (5.23)$$

where we used  $g_{rr} = 1/(f r^2)$  and  $\sqrt{-g} = e^{2(\Phi - \Phi_0)} = 1/r$ . Hence, in the two dimensional case the dilaton  $\Phi$  plays again the role of the 4d spherical coordinates, now in the wave equation.

As in the  $d \geq 4$  cases, we separate variables

$$\psi(r, t) = \psi_\omega(r) e^{i\omega t}. \quad (5.24)$$

The equation for  $\psi_\omega$  is:

$$(\partial_r r^2 f \partial_r + \omega^2 f^{-1} - m^2) \psi_\omega = 0. \quad (5.25)$$

---

<sup>14</sup>This can be obtained, for instance, as (part of) a low-energy effective action of an heterotic string in two dimensions (for a review, see [1]).

Again, we define a coordinate  $r^*$ ,

$$dr^* = \frac{dr}{rf(r)}, \quad (5.26)$$

and a new field variable

$$\psi^* := \sqrt{r}\psi, \quad (5.27)$$

such that eq. (5.25) turns into:

$$[-\partial_{r^*r^*} + V_{\text{eff}}(r^*) - \omega^2] \psi_\omega^* = 0. \quad (5.28)$$

The effective potential is now

$$V_{\text{eff}}(r^*) = \Delta V_{\text{eff}} + fm^2, \quad (5.29)$$

where

$$\Delta V_{\text{eff}} = \frac{1}{2} \sqrt{r} f \partial_r (\sqrt{r} f). \quad (5.30)$$

Next we inspect the behavior of the wave equation (5.25) near the singularity of the 2d RN-like black hole. When  $Q \neq 0$ :

$$\begin{aligned} & \frac{1}{Q^2} (\partial_r r^2 f \partial_r + \omega^2 f^{-1} - m^2) \psi_\omega = \\ & \left[ (1 + \dots) \partial_{rr} + O(r^0) \partial_r - \frac{m^2}{Q^2} + (1 + \dots) \frac{r^2 \omega^2}{Q^4} \right] \psi_\omega = 0, \end{aligned} \quad (5.31)$$

where “...” stand for higher orders in  $r$ . As in the 4d case (3.6), this equation is regular at  $r = 0$  for every  $\omega$ . Moreover, near  $r \sim 0$  we have

$$r^* \cong \frac{r^2}{2Q^2} \quad (5.32)$$

and hence

$$V_{\text{eff}}(r^*) \cong -\frac{3}{16 r^* 2}. \quad (5.33)$$

On the other hand, for  $Q = 0$  – the Schwarzschild-like 2d black hole – the equation for  $\psi_\omega$  is:

$$\begin{aligned} & -\frac{1}{2Mr} (\partial_r r^2 f \partial_r + \omega^2 f^{-1} - m^2) \psi_\omega = \\ & \left[ (1 + \dots) \partial_{rr} + \frac{(1+\dots)}{r} \partial_r + \frac{m^2}{2Mr} + (1 + \dots) \frac{\omega^2}{4M^2} \right] \psi_\omega = 0. \end{aligned} \quad (5.34)$$

Again, as in the 4d case (3.9), it is not regular at the singularity, but instead it is regular-singular. In the uncharged case, to leading order near  $r \sim 0$  we have

$$r^* \cong -\frac{r}{2M} \quad (5.35)$$

and hence

$$V_{\text{eff}}(r^*) \cong -\frac{1}{4 r^* 2}. \quad (5.36)$$

As discussed in previous sections, the solutions to high frequency scattering wave equations (5.28) are given in terms of Bessel functions, which depend on the effective potential. In



the charged case we read the order of the relevant Bessel function from (5.33) and appendix D:

$$|n| = \frac{1}{4} , \quad (5.37)$$

and hence at high energies we find (5.12):

$$|T| = |R| = \frac{1}{\sqrt{2}} . \quad (5.38)$$

On the other hand, for the uncharged case, from (5.36) and (5.12) we read:

$$\begin{aligned} n &= 0 \\ |R| &= 1 , \quad T = 0 . \end{aligned} \quad (5.39)$$

To summarize, we see that the features of the 2d black holes discussed in this subsection are very similar to the 4d case.

The 2d background (5.20) is also an exact Conformal Field Theory (CFT) background in string theory; in [4] it was obtained from a family of  $\frac{SL(2, \mathbb{R}) \times U(1)}{U(1)}$  quotient CFT sigma models by a Kaluza-Klein reduction<sup>15</sup>. In string theory one is forced to include the regions beyond the singularity [32] (this is argued, for instance, by using T-duality; for a review, see [33]). The structure of the parent  $SL(2, \mathbb{R})$  group allows one [4] to find the exact solutions to the wave equation<sup>16</sup>. In particular, it gives the exact reflection coefficient

$$|R(\omega)|^2 = \frac{\cosh\left(\frac{r_-\omega}{r_+ - r_-}\right) \cosh(\omega)}{\cosh\left(\frac{r_+\omega}{r_+ - r_-}\right)} , \quad (5.40)$$

where  $\omega$  is proportional to the energy of a massless particle scattered from the region beyond the black hole singularity, and  $r_{\pm}$  are the locations of the event and Cauchy horizons:

$$r_{\pm} = M \pm \sqrt{M^2 - Q^2} . \quad (5.41)$$

Indeed, for the charged case  $|R|^2 \rightarrow \frac{1}{2}$  in the limit  $\omega \rightarrow \infty$ , and for the uncharged case  $|R|^2 = 1$  for every energy. These results are in agreement with (5.38) and (5.39), respectively.

## 6. Adding perturbations

Until now we assumed that  $\phi$  was a scalar field with no mass, no charge, no back-reaction and no other interactions beyond minimal coupling to gravity. Now we will check whether our result that the time evolution is well-defined is disrupted by any of these perturbations. To our surprise we do not encounter any problem.

---

<sup>15</sup>In the bosonic case it is a semi-classical approximation, while in the superconformal extension this background is claimed to be exact [31].

<sup>16</sup>Scattering waves are determined from vertex operators in the  $SL(2, \mathbb{R})$  CFT. Those are given by matrix elements in a unitary representation of the group. Equivalently, these are solutions to the Laplace equation (5.23), which in this case is a solvable hypergeometric equation.

## 6.1 Mass and charge

Adding a mass  $m$  and charge  $q$  for the field  $\phi$  is completely captured by the form of the geodesic potential (2.19), namely one has

$$\begin{aligned} V_{\text{eff}}^{\text{wave}} &= \tilde{V}_{\text{eff}}^{\text{geodesic}} + \Delta V_{\text{eff}} \\ \tilde{V}_{\text{eff}}^{\text{geodesic}} &= \left( \frac{l(l+d-3)}{r^2} + m^2 \right) f(r) - \left( E - \frac{qQ}{r^{d-3}} \right)^2 \\ \Delta V_{\text{eff}} &= \frac{d-2}{2} \frac{f}{r^{(d-2)/2}} \partial_r (r^{(d-4)/2} f) \end{aligned} \quad (6.1)$$

where  $\tilde{V}_{\text{eff}}^{\text{geodesic}}$  is simply  $V_{\text{eff}}^{\text{geodesic}}$  from (2.19) with the substitutions  $l^2 \rightarrow l(l+d-3)$  and  $E \rightarrow \omega$ , and  $\Delta V_{\text{eff}}$  is the same as in the zero-mass zero-charge case (3.16,5.8).

Our analysis relied on the leading terms near  $r \sim 0$ , which we will now find to dominate over the added perturbations. For  $Q \neq 0$  these are  $1/r^{4d-10}$  from  $\Delta V_{\text{eff}}$  and  $l^2/r^{2d-4}$  from  $\tilde{V}_{\text{eff}}^{\text{geodesic}}$ . Since both  $m$  and  $q$  contribute at order  $1/r^{2d-6}$ , they are irrelevant near the singularity (for  $d \geq 4$ ). Moreover, one can confirm that the form of the subleading terms still conform with (5.4) and hence there are no log pieces in the solutions.

Note however that since for  $q \neq 0$  one cannot solve for  $\omega^2$  in the wave equation and view it as eigen-values of some operator, any operator approach and considerations of self-adjointness (see section 7) would need to be changed.

Finally, for  $Q = 0$  we might as well take  $q = 0$  and the leading terms are  $1/r^{2d-4}$  from  $\Delta V_{\text{eff}}$  and  $l^2/r^{d-1}$  from  $\tilde{V}_{\text{eff}}^{\text{geodesic}}$ , while  $m$  contributes at  $1/r^{d-3}$  and is again irrelevant.

## 6.2 Interactions

We may add non-quadratic terms to the action, namely adding terms non-linear in  $\phi$  to the wave equation. Much of our previous analysis, especially the separation of variables relied on linearity, hence we should reconsider it, starting from the non-linear wave equation

$$0 = \square \phi - g U(\phi) , \quad (6.2)$$

where  $g$  is a coupling constant and  $U(\phi)$  is a non-linear potential term. One can attempt to solve this equation by perturbation theory with  $g$  being the small parameter, namely one expands

$$\phi = \sum_j g^j \phi^{(j)} . \quad (6.3)$$

We start at zeroth order with a solution  $\phi^{(0)}$  to the linearized equation

$$\square \phi^{(0)} = 0 \quad (6.4)$$

and consider whether the first correction is regular at  $r = 0$ . The first correction satisfies

$$\square \phi^{(1)} = g U(\phi^{(0)}) . \quad (6.5)$$

In order to solve this equation we separate the angular and time variables

$$f^{-1} \square_{\omega l} \phi_{\omega l}^{(1)} = g f^{-1} \left[ U(\phi^{(0)}) \right]_{\omega l} . \quad (6.6)$$

Since  $\phi^{(0)}$  is regular by assumption, so are the components  $[U(\phi^{(0)})]_{\omega l}$ . This is a non-homogeneous ordinary (second order) differential equation. A solution in the vicinity of the singularity may be obtained by Taylor expanding the equation (see also section 7). The homogeneous solutions are the smooth  $\phi_{\omega l}^{(0)}$ , while the non-homogenous term added to (5.3) is  $O(f^{-1}(r))$  and hence it is subleading and does not change our ability to obtain a (univalued) solution. This will happen at higher orders in  $g$  as well.

### 6.3 Back-reaction for RN in $d \geq 4$

So far we worked in the linear approximation where one neglects the back-reaction of the scalar field on the background geometry. Let us check whether including the back-reaction disrupts our result, namely whether we can find any obstruction for the solutions to the linear equation from being extended to solutions for the full non-linear system of background plus scalar field. Our analysis will be limited to lowest order back-reaction, and we shall not cover all cases, but the indications are that these solutions do survive back-reaction.

Let us define a small parameter  $\epsilon$  such that  $\phi$  is first order in  $\epsilon$ . Then at second order the background may change – the metric due to a  $T_{\mu\nu}$  source, and the electromagnetic (EM) field due to the charge associated with  $\phi$ . For simplicity we may consider  $\phi$  to be neutral. Since the metric is singular to start with, we cannot use the straight-forward criterion that the background remains regular after back-reaction. A conservative view would be to continue and look at third order whether the changes in  $\phi$  as a result of the changes in the background make it singular. Another approach is to require that the singularity in the metric does not become worse after back-reaction. The latter has the advantage that one can stop at second order.

Moreover, for a charged black hole we can even save us the work of computing the second order by the following observation. Let us compare the stress-energy tensor of the scalar field with that of the EM field, namely the background source. The action for gravity + EM + an uncharged scalar field is

$$S = \int d^d x \sqrt{-g} \left( R - \frac{1}{4} F^2 - g^{\mu\nu} \partial_\mu \phi \partial_\nu \phi - m^2 \phi^2 \right), \quad (6.7)$$

where  $g_{\mu\nu}$  is the metric,  $F$  the field strength and  $\phi$  an uncharged scalar field of mass  $m$ . The stress tensors of the gauge and scalar fields are

$$\begin{aligned} T_{\mu\nu}^{(F)} &= \frac{1}{2} F_{\mu\rho} F_{\nu\sigma} g^{\rho\sigma} - \frac{1}{8} g_{\mu\nu} F^2 \\ T_{\mu\nu}^{(\phi)} &= \partial_\mu \phi \partial_\nu \phi - \frac{1}{2} g_{\mu\nu} [(\partial\phi)^2 + m^2 \phi^2] \end{aligned} \quad (6.8)$$

We start by comparing the scalar quantities

$$\begin{aligned} (\partial\phi)^2 &= \partial_r \phi \partial_r \phi g^{rr} \sim \frac{1}{r^{2(d-3)}} \\ (F^2) &= F_{rt} F_{rt} g^{rr} g^{tt} \sim \frac{1}{r^{2(d-2)}} \end{aligned} \quad (6.9)$$

where we use the background (5.1) and the property that  $\phi$ ,  $\partial_r\phi$  are regular at the singularity. We see that close to the singularity the scalar field seems to add a negligible source on top of the one from the EM field.

We now proceed to compare all components

$$\begin{aligned}
T_{rr}^{(F)} &\sim \frac{1}{r^2} & T_{rr}^{(\phi)} &\sim 1 \\
T_{tt}^{(F)} &\sim \frac{1}{r^{2(2d-5)}} & T_{tt}^{(\phi)} &\sim \frac{1}{r^{4(d-3)}} \\
T_{rt}^{(F)} &= 0 & T_{rt}^{(\phi)} &\sim 1 \\
T_{\theta\theta}^{(F)} &\sim \frac{1}{r^{2(d-3)}} & T_{\theta\theta}^{(\phi)} &\sim \frac{1}{r^{2(d-4)}}
\end{aligned} \tag{6.10}$$

We see that indeed for the  $rr$ ,  $tt$  and  $\theta\theta$  components  $T_{\mu\nu}^{(\phi)} \sim r^2 T_{\mu\nu}^{(F)}$  is negligible, while  $T_{rt}^{(\phi)}$  is regular. Altogether we consider this to be strong evidence that back-reaction is weak and does not change the smoothness of the solutions.

For a charged field  $\phi$  the simple argument above does not seem to work. In principle one should determine the back-reaction to the metric and gauge field and whether they are more or less singular than the original background. A preliminary analysis turned out to be involved, and so we did not reach any conclusions for this case. For similar reasons we do not discuss the back-reaction to the negative-mass Schwarzschild either.

#### 6.4 Back-reaction for the 2d black-hole

In two dimensions, the action for an uncharged scalar field coupled to the metric and dilaton is (see subsection 5.2):

$$S = \int d^2x \sqrt{-g} e^{-2\Phi} \left( R + 4g^{\mu\nu} \partial_\mu \Phi \partial_\nu \Phi - \frac{1}{4} F^2 - \lambda - g^{\mu\nu} \partial_\mu \psi \partial_\nu \psi - m^2 \psi^2 \right), \tag{6.11}$$

where  $g_{\mu\nu}$  is the string frame metric,  $\Phi$  the dilaton,  $F$  is the field strength of an Abelian gauge field  $A$ ,  $\psi$  is the scalar field (to distinguish it from the dilaton) and  $\lambda$  is the cosmological constant.

Using the background (5.20) and the property that  $\psi$ ,  $\partial_r\psi$  are regular at the singularity, we find the following behavior of the scalar stress tensor (6.8) near the singularity

$$\begin{aligned}
e^{2\Phi} T_{rr}^{(\psi)} &\sim 1 \\
e^{2\Phi} T_{tt}^{(\psi)} &\sim \frac{1}{r^2} \\
e^{2\Phi} T_{rt}^{(\psi)} &\sim 1
\end{aligned} \tag{6.12}$$

The dilaton stress tensor is

$$e^{2\Phi} T_{\mu\nu}^{(\Phi)} = 4\nabla_\mu \nabla_\nu \Phi - 4g_{\mu\nu} \left( \nabla^2 \Phi - (\partial\Phi)^2 - \frac{1}{4}\lambda \right) \tag{6.13}$$

and has the following leading behavior near the singularity

$$\begin{aligned}
e^{2\Phi} T_{rr}^{(\Phi)} &\sim \frac{1}{r^2} \\
e^{2\Phi} T_{tt}^{(\Phi)} &\sim \frac{1}{r^4} \\
e^{2\Phi} T_{rt}^{(\Phi)} &= 0
\end{aligned} \tag{6.14}$$

Again, there is no strong back-reaction to the metric, since component-wise each component of  $T_{\mu\nu}^{(\psi)}$  is either subleading to  $T_{\mu\nu}^{(\Phi)}$  or regular.

To check the back-reaction to the dilaton, we define

$$\chi = e^{-\Phi} \quad , \quad (6.15)$$

in terms of which the action becomes

$$S = \int d^2x \sqrt{-g} \left[ 4g^{\mu\nu} \partial_\mu \chi \partial_\nu \chi + \chi^2 \left( R - \frac{1}{4} F^2 - \lambda - g^{\mu\nu} \partial_\mu \psi \partial_\nu \psi - m^2 \psi^2 \right) \right] . \quad (6.16)$$

The equation of motion for  $\chi$  is

$$4\Box\chi - \left( R - \frac{1}{4} F^2 - \lambda - g^{\mu\nu} \partial_\mu \psi \partial_\nu \psi - m^2 \psi^2 \right) \chi = 0 \quad , \quad (6.17)$$

where  $\Box$  is the Laplacian without the dilaton. In principle, we should expand the solution to (6.17) to second order in the perturbation and compare the correction to its initial value<sup>17</sup>. However, just like for the metric, we recognize that the new source for  $\chi$ ,  $(g^{\mu\nu} \partial_\mu \psi \partial_\nu \psi - m^2 \psi^2)$ , is negligible at the singularity relative to the background sources  $(R - \frac{1}{4} F^2)$ . Therefore, we do not expect a strong back-reaction for the dilaton either. Summarizing, we find indications for a weak back-reaction near the singularity of the 2d charged black-hole.

## 7. General conditions for resolution of a singularity

### 7.1 Uniqueness of decomposition and natural boundary conditions

In order for the ‘‘singularity smoothing’’ procedure which we defined in section 3 to make sense we need the existence and uniqueness of decomposition of any initial condition into a linear combination of eigen-functions  $\phi_\omega$ . We know that Hermitian operators have this property, namely their eigen-functions form a basis of function space. Thus we are interested in representing the radial equation  $\Box_{\omega l} \phi_\omega = 0$  through an operator and studying its Hermiticity, and so we define the operator  $L$  by

$$\begin{aligned} f \Box_{\omega l} &= \omega^2 - L[\partial_r, r] \\ L &:= -\frac{f}{r^2} \partial_r f r^2 \partial_r + \frac{f l(l+1)}{r^2} \end{aligned} \quad (7.1)$$

and we specialize back to 4d for definiteness. We note that  $L$  is not regular at  $r = 0$  even for RN but only due to an overall factor of  $f^2$  relative to the regular radial equation  $f^{-1} \Box_{\omega l}$  (3.5). One may wonder whether the decomposition property would nevertheless hold for  $L$ . This will be answered in the negative as we shall show that the functions  $\phi_\omega$  do not span all possible functions.

---

<sup>17</sup>At zero order we have  $\chi = \chi_0 \sqrt{r}$  (5.20, 5.21). The second solution to (6.17) is subleading near  $r = 0$ , so turning it on at higher orders would not change the result.

Since the differential equation (3.5) is smooth at  $r = 0$  one can Taylor expand the equation and solutions

$$\phi_\omega(r) = \sum_{j=0}^{\infty} \phi_\omega^{(j)} r^j . \quad (7.2)$$

Substituting this in the differential equation transforms it into a recurrence equation for the Taylor coefficients  $\phi_\omega^{(j)}$ .

For RN one notes that the coefficient of  $\omega^2$  is  $f^{-2}$  which is  $O(r^4)$  and hence the recurrence equation is  $\omega$ -independent up to order  $O(r^3)$  (inclusive) where  $\phi_\omega^{(5)}$  is determined. Among the first 6 Taylor coefficients  $\phi_\omega^{(0)}, \dots, \phi_\omega^{(5)}$  the first two may be considered to be initial conditions for the recurrence equation and the other four may be considered to be a function of them. In other words we find 4  $\omega$ -independent linear relations among  $\phi_\omega^{(0)}, \dots, \phi_\omega^{(5)}$ . Owing to the  $\omega$ -independence of these relations they continue to hold for any function which can be expressed as a linear combination

$$\phi_i = \int d\omega (\phi_+(\omega) + \phi_-(\omega)) \phi_\omega(r) , \quad (7.3)$$

where  $\phi_\pm(\omega)$  are arbitrary coefficients. This means that there are 4 conditions on the first 6 coefficients of any function in  $\text{span}(\phi_\omega)$ .

For Schwarzschild the phenomenon is similar but the details are different. We have  $f^{-2} = O(r^2)$  and hence the recurrence relation is free up to (and including) the 4th coefficient  $\phi_\omega^{(3)}$ . Since we consider only the regular solutions then the recurrence relation requires a single initial condition  $\phi_\omega^{(0)}$  while  $\phi_\omega^{(1)}, \dots, \phi_\omega^{(3)}$  may be considered to be an  $\omega$ -independent function of it, and hence there are necessarily 3 conditions on the first 4 Taylor coefficients of any function in  $\text{span}(\phi_\omega)$ .

We see that  $\text{span}(\phi_\omega)$  does not contain all functions, but rather there are constraints on the initial conditions at  $r = 0$ . This is why we required the time-evolution to be well-defined only for wave packets prepared far away, but otherwise arbitrary. We expect that once the domain of  $L$  is correctly defined it will be Hermitian and uniqueness of decomposition will hold and consequently the uniqueness of time evolution. The mathematical term that we expect to hold is that  $L$  is “essentially self-adjoint” namely that it has a unique Hermitian (i.e. self-adjoint) extension (see [34] for a text book and [10, 8]).

#### *Initial conditions at $r=0$*

Let us find some necessary boundary conditions at  $r = 0$  in response to the “non-span” property just discussed. Since  $L$  defined in (7.1) is singular at  $r = 0$   $\partial_{tt}$  may be ill-defined (which reflects the singular nature of the wave equation (3.2)). Since  $\phi$  is finite at  $r = 0$  we need  $\partial_{tt}\phi$  to be finite as well <sup>18</sup> and thus we clearly need

$$L\phi = \text{finite} \quad (7.4)$$

where  $\phi$  can be either of the initial conditions  $\phi_i, \dot{\phi}_i$ .

---

<sup>18</sup>In the rest of this subsection “finite” should be understood to mean “finite at  $r = 0$ .”

For RN from the leading behavior for  $f_{\text{RN}}$  (2.2), we get that for a regular and generic  $\phi$  the Laurent expansion of  $L\phi$  starts at degree  $(-4)$ , and thus eq. (7.4) represents 4 conditions (for degrees  $-4 \leq \text{deg} \leq -1$ ). Moreover, if we Taylor expand  $\phi = \sum_{j=0}^{\infty} \phi^{(j)} r^j$  then at order  $\text{deg}$  the largest  $j$  for which  $\phi^{(j)}$  appears in the equation is  $j = \text{deg} + 6$ , and so we have 4 (linear, homogeneous) conditions for the 6 coefficients  $\phi^{(0)}, \dots, \phi^{(5)}$ . These are actually the conditions found in the paragraph around eq. (7.2), which limit our choice of initial conditions in the vicinity of  $r = 0$ .

Similarly, for Schwarzschild (7.4) represents 3 conditions (for degrees  $-3 \leq \text{deg} \leq -1$ ) among the first 4 Taylor coefficients which agree with the findings in the paragraph after eq. (7.2).

However, there are additional requirements: the constraint (7.4) must be compatible with the time evolution according to the wave equation

$$L\phi = -\partial_{tt}\phi \tag{7.5}$$

namely we must require

$$\partial_{tt}[L\phi] = \text{finite} \tag{7.6}$$

By the wave equation (7.5) this is equivalent to

$$L^2\phi = \text{finite} \tag{7.7}$$

This gives 4 additional conditions (in addition those of (7.4)) involving the first 12 Taylor coefficients for RN and 3 additional conditions for the first 8 Taylor coefficients for Schwarzschild.

Now we may readily generalize, and find

**Necessary boundary condition:**

$$L^n\phi = \text{finite} \quad \forall n \geq 1 \tag{7.8}$$

(at  $r = 0$ ).

This condition holds both for RN and Schwarzschild and is explicitly compatible with time evolution. Note that it can also be interpreted as  $\partial_{tt}^n\phi = \text{finite} \quad \forall n \geq 1$ . It is plausible to us that this condition is not only necessary but also sufficient for a unique time evolution as well since showing that  $\phi$  has finite time derivatives of any order at the initial moment of time comes close to providing a well-defined time evolution, but we shall not attempt to pursue this point.

As we already mentioned, the boundary conditions (7.8) are automatically satisfied for characteristic b.c. (at past null infinity) and more generally b.c. which vanish at a neighborhood of  $r = 0$ .

Another perspective is to consider a numerical computer implementation of this time evolution. One may either have no grid points at  $r = 0$  in which case the time evolution is well-defined, or put a grid point at  $r = 0$  and find its time increment as a limit of the

time increments of neighboring points. The singularity will tend to “expand” numerical errors, but those should be possible to tame by decreasing the grid spacing. It would be interesting to analyze this further and/or to perform the implementation and determine the behavior at  $r = 0$ .

## 7.2 General conditions for wave-regularity

Having shown that Reissner-Nordström is wave-regular allowing for transmission across the singularity, we would like to abstract the general conditions on a spacetime to have such a resolution.

The crucial property of the RN singularity is that the two solutions  $\phi_\omega$  have a unique continuation across  $r = 0$ , while *a priori* there could have been multi-valued functions such as the log’s which appear in the Schwarzschild case. Hence a wave packet constructed from the  $\phi_\omega$  has a prospect of crossing the singularity in a well-defined manner. This is true not only in 4d RN where the time-separated ODE is regular but also for  $d > 4$  RN where the ODE becomes regular-singular rather than smooth, but nevertheless the two characteristic exponents are integral and there are no log pieces so that the functions  $\phi_\omega$  are univalued in the vicinity of the singularity. The condition on the characteristic exponents can be generalized to allow for a reparameterization of coordinate  $r \rightarrow \tilde{r} \sim r^{c_1}$  and a linear redefinition of the field  $\phi \rightarrow r^{c_2} \phi_\omega$  for some constants  $c_1, c_2$ . In general  $\phi_\omega$  can be series expanded as  $\phi_\omega = \tilde{r}^\rho \sum_{k=0}^{\infty} \phi^{(k)} \tilde{r}^{k\Delta}$  where  $\rho = \rho_{1,2}$  is one of the two characteristic exponents and  $\Delta$  is the “series step-size” ( $\Delta = 1$  when the functions in the differential equation are meromorphic) and  $\phi^{(k)}$  are some constants. The quantity  $(\rho_1 - \rho_2)/\Delta$  is invariant under the double transformation above, and hence there exists a transformation such that all three  $\rho_1, \rho_2$  and  $\Delta$  are integral and the function is univalued exactly if the ratio above is rational.

We summarize the above by

**Necessary general condition:** the “eigen-functions”  $\phi_\omega$  should be univalued in the vicinity of the singularity. This is equivalent to:

- The equation for  $\phi_\omega$  is either regular or regular-singular. If it is regular-singular we also require the next items:
- The difference of characteristic exponents is commensurate with the “series step-size” (defined in the previous paragraph)

$$\frac{\rho_2 - \rho_1}{\Delta} \in \mathbb{Q} . \tag{7.9}$$

- There are no log pieces in the solutions.



## 8. Summary and discussion

In this paper we saw that physical predictability can be restored in the neighborhood of the charged (RN) black-hole singularity as well as negative mass Schwarzschild, once one considers waves rather than particles. For RN this is done by gluing two spacetimes over the time-like singularity, thereby adding another asymptotic region. An observer at infinity in the additional region views a spacetime with a negative mass. Several alternatives exist for the total Penrose diagram depending on the relative size of  $M^2$  and  $Q^2$ . This singularity appears to have the physical nature of a beam splitter.

For negative-mass Schwarzschild there is a natural “regularity” boundary condition at the singularity cutting off spacetime there, and thus it can be physically interpreted as a perfectly reflecting mirror.

We subjected this picture to several tests by adding perturbations in section 6. Considering a field with both mass and charge we found that such terms are subleading at the neighborhood of the singularity. Considering added interactions the field equation becomes non-linear and we were satisfied in confirming that there is no obstruction (such as creating a divergence) in extending the linear solutions to next order. Similarly we then considered the effect of non-linearities from back-reaction, and found that in some cases a simple argument protects the regularity of  $\phi$  at the next order. Altogether the results were surprisingly resilient to perturbations.

It would be interesting to perform some additional tests and generalizations:

- Study fields with other spin. Of particular interest are the electromagnetic and gravitational fields, and also the Dirac  $s = 1/2$  field. A preliminary investigation of the electromagnetic and gravitational fields in  $d=4$  indicates that their polar modes behave just as scalar fields, i.e. 75% reflection and 25% transmission for high energy at fixed  $l$ . The axial modes appear to be more subtle, however.
- Study other backgrounds such as extreme RN and rotating black-holes.

Rotating black-holes deserve a special discussion here. They may be linked to our work in two different ways. First, the motivation to the present analysis partly emerges from the desire to explore the physical phenomena that may take place deep inside realistic rotating black holes. From this point of view the spherical charged black hole serves as a toy model for the more complicated, non-spherical, spinning black hole. In the second link we can employ the spinning black holes to test the singularity-resolution approach developed here. In the Kerr-Newman solution the  $r = 0$  singularity forms a ring rather than a hypersurface. Once the field is decomposed into spheroidal-harmonic modes, the field equation for each mode is perfectly regular at  $r = 0$ , hence there is no doubt about the proper continuation. Now, when the spin parameter  $a$  is taken to vanish, the ring’s radius shrinks to zero, and the spacetime becomes RN. One may therefore *define* the RN extension of the field beyond the  $r = 0$  singularity to be the limit  $a \rightarrow 0$  of the corresponding field in the Kerr-Newman case. The obvious question is, therefore: does this procedure yield exactly the same extension as that constructed above? At least for a scalar field in 4d RN

the answer is found to be positive. It still remains to check whether this is also the case in the  $Q = 0$  case. Namely, in the uncharged Kerr case, when  $a \rightarrow 0$  and the spacetime becomes Schwarzschild, does one recover the full-reflection b.c. advocated above? This still needs to be verified.

We would like to mention several other issues at the classical level:

- In all of our examples one of the spacetimes has a negative mass and a globally-naked singularity. Such physical objects raise problematic issues, and we name only a few: anti-gravity, acceleration reversed to force, and also inconsistency of their construction with the Cosmic Censorship conjecture (see “Perspectives on  $r < 0$ ” in section 2).

It would be interesting to determine whether Nature allows the actual construction of any spacetime with a *wave-regular timelike singularity*. The mechanism that immediately suggests itself would be to reconsider a gravitational collapse of a charged spherical shell (in the positive-mass universe), leading to a RN black-hole geometry (outside the collapsing object). However, the instability of the inner horizon raises some doubts about whether the RN-like  $r = 0$  singularity will indeed form in this process.

- Implications for *Cosmic Censorship*. At the very least it shakes its rationale since given “reasonable” initial conditions Cosmic Censorship is supposed to “protect us” from loss of predictability, namely of losing unique time evolution, by forbidding naked singularities, but here we see that such singularities may not mean the loss of predictability after all.
- Since for RN we advocate a picture where there are two spacetimes which are consistently glued at the singularity — and since a macroscopic measuring device cannot cross the singularity (at best it will bounce back, but it may also be destroyed by tidal forces, or be “beam-splitting,” in the worse case) one may take *two different points of view* on the physics corresponding to either of the two observers on the two sides of the singularity. Namely, the story of the resolution of each singularity will be told in two different versions corresponding to the two observers (this applies to both types of RN spacetime, namely  $|Q| < |M|$  and  $|Q| > |M|$  – see figures 2,5).

Going beyond classical GR there are open questions as to the quantum gravity consistency and properties:

- We must note that our wave equation is outside its *domain of validity* near the singularity due to the presence of high curvature. However, a preliminary analysis shows that quantum corrections do not produce essential singularities in the equations and start altering the field only at a Planck (proper) distance from the singularity.
- Semi-classical quantization and Hawking evaporation (under study).

- As one passes to the quantum theory one may suspect that the pathologies associated with negative-mass spaces to only grow worse. Therefore, we need to be very cautious in discussing possible implications for “*legitimizing*” *spacetimes* with such singularities as possible solitons, namely which spacetimes should be considered to contribute to the path integral as admissible saddle points. Here we took an open-minded approach of exploration and we hope that the various interesting issues which get raised will be studied further.

### Acknowledgements

We would like to thank O. Aharony, J. Bekenstein, M. Berkooz, G. Gibbons, J. Katz, D. Kazhdan, N. Itzhaki, D. Kutasov, M. Rozali and R.M. Wald for discussions. This work is supported in part by the Israeli Science Foundation. AG is supported in part by the Israel Academy of Sciences and Humanities – Centers of Excellence Program, the German-Israel Bi-National Science Foundation, and the European RTN network HPRN-CT-2000-00122. BK is supported in part by the Israeli Science Foundation and by the Binational Science Foundation BSF-2002160. AS is supported in part by the Horowitz Foundation.

### A. Kruskal-Szekeres coordinates

For completeness, we recall here the derivation of the metrics in the Kruskal-Szekeres coordinates and the definition of the functions  $g(r)$  which are mentioned in the text and are used to implicitly define  $r$  in these coordinates.

First one defines the “tortoise” coordinate  $r^*$  by

$$dr^* := \frac{dr}{f} . \tag{A.1}$$

$r^*$  diverges on horizons but is finite at  $r = 0$ . Then one passes to light-cone coordinates

$$\begin{aligned} v &:= t + r^* \\ u &:= t - r^* \end{aligned} \tag{A.2}$$

and finally in the neighborhood of a horizon with surface gravity  $\kappa$  (for Reissner-Nordström we have  $\kappa_{\pm} = (r_+ - r_-)/(2r_{\pm}^2)$  while for Schwarzschild  $\kappa = 1/(2r_0)$ ) the Kruskal-Szekeres coordinates are given by

$$\begin{aligned} V &:= \pm \exp(\pm \kappa v) \\ U &:= \pm \exp(\pm \kappa u) \end{aligned} \tag{A.3}$$

and the sign inside the exponent is chosen such that the horizon is located at  $UV = 0$ , namely it is X-shaped.

In these coordinates the metric is given by

$$ds^2 = -\frac{f}{\kappa^2 g} dU dV + r^2 d\Omega^2 , \tag{A.4}$$

where the function  $g(r)$  is defined by

$$g(r) := \exp(\pm 2 \kappa r^*) \quad (\text{A.5})$$

and the sign is chosen to be the same as that for  $V$  in (A.3).  $r$  is not a coordinate anymore, but rather it is implicitly defined in terms of the  $U, V$  coordinates by

$$-UV = g(r) . \quad (\text{A.6})$$

Note that by construction  $g(r)$  has a zero at the horizon and thus the horizon is explicitly smooth in these coordinates since in the prefactor of  $dU dV$  the zero in  $f$  gets cancelled against the zero in  $g$ .

In Reissner-Nordström there are two horizons at  $r_{\pm}$ , and accordingly two Kruskal-Szekeres-like planes for  $(U_{\pm}, V_{\pm})$ , and two functions  $g_{\pm}(r)$ . The “upper plus” quadrant ( $U_+, V_+ > 0$ ) is glued to the “lower minus” quadrant ( $U_-, V_- < 0$ ) according to

$$\begin{aligned} V_+^{1/\kappa_+} &= (-V_-)^{1/\kappa_-} \\ U_+^{1/\kappa_+} &= (-U_-)^{1/\kappa_-} \end{aligned} \quad (\text{A.7})$$

and similarly one may continue and glue the upper minus quadrant to another copy of the plus plane, creating the maximal analytic extension of Reissner-Nordström which consists of an infinite chain of alternating plus and minus planes.  $g_{\pm}(r)$  are given by (see figure 1)

$$\begin{aligned} g_+(r) &= \left( \frac{r}{r_+} - 1 \right) \left( \frac{r}{r_-} - 1 \right)^{-\frac{\kappa_+}{\kappa_-}} \exp(2 \kappa_+ r) \\ g_-(r) &= \left( 1 - \frac{r}{r_-} \right) \left( 1 - \frac{r}{r_+} \right)^{-\frac{\kappa_-}{\kappa_+}} \exp(-2 \kappa_- r) \end{aligned} \quad (\text{A.8})$$

While for Schwarzschild we have (see figure 3)

$$g_{\text{schw}}(r) = \left( \frac{r}{r_0} - 1 \right) \exp(r/r_0) . \quad (\text{A.9})$$

Finally, in order to get the Penrose diagram (see figures 2,4,5) one customarily takes the conformal transformation

$$\begin{aligned} U_P &= \text{tg}^{-1}(U) \\ V_P &= \text{tg}^{-1}(V) \end{aligned} \quad (\text{A.10})$$

although any other transformation which maps the real line to an interval is admissible.

## B. Regular singularities of ordinary differential equations

Let us briefly recall the definitions. A linear second order differential equation

$$[a(r) \partial_{rr} + b(r) \partial_r + c(r)] \phi = 0 \quad (\text{B.1})$$

is regular-singular at a point  $r_0$ , which we will assume without loss of generality to be  $r_0 = 0$ , if after normalization such that  $a(0) = 1$  there are singularities at  $r = 0$  in  $b(r)$  or  $c(r)$  of limited type:  $b(r)$  may have at most a first order pole, and  $c(r)$  at most a second order pole. This guarantees that the solutions will have at most poles or branch cuts at  $r = 0$  but not an essential singularity. More specifically the two solutions have the leading behavior

$$\phi_{1,2} \sim r^{\rho_{1,2}}, \quad (\text{B.2})$$

where  $\rho_{1,2}$  are called the characteristic exponents, and they are the solutions to the quadratic equation

$$a(r_0)\rho(\rho - 1) + b(r_0)r\rho + c(r_0)r^2 = 0 \quad (\text{B.3})$$

gotten from substituting the leading behavior above into the equation. When  $\rho_1 = \rho_2 = \rho$  the leading behavior is  $\phi_1 = r^\rho$ ,  $\phi_2 = r^\rho \log(r)$ . Finally, one can expand the solutions into a series  $\phi = r^\rho \sum_{j=0}^{\infty} \phi^{(j)} r^j$  where  $\phi^{(j)}$  are some constants, except that in the case when  $\rho_2 - \rho_1$  is a positive integer  $\phi_1$  may contain also a piece proportional to  $\log(r)$   $\phi_2$  and thus contains a log.

### C. Basis functions for the characteristic formulation

Here we define the basis functions  $\phi_{(\omega_v, 0)}^*$ ,  $\phi_{(0, \omega_u)}^*$  for the characteristic formulation (see subsection 3.4). Since the radial equation is a second-order ODE, the radial functions  $\phi_\omega^*(r^*)$  for a given  $\omega$  form a two-parameter family. Owing to the asymptotic behavior of the radial functions, Eq. (3.23), we may choose two basis functions  $\phi_{\omega(1,0)}^*(r^*)$  and  $\phi_{\omega(0,1)}^*(r^*)$ , defined as follows:  $\phi_{\omega(1,0)}^*(r^*)$  is the radial function which at  $r^* \rightarrow +\infty$  (the inner horizon) has the asymptotic form

$$\phi_{\omega(1,0)}^* \cong T(\omega)\exp(-i\omega r^*)$$

and at  $r^* \rightarrow -\infty$  (the negative- $r$  asymptotically-flat region) has the asymptotic form

$$\phi_{\omega(1,0)}^* \cong \exp(-i\omega r^*) + R(\omega)\exp(+i\omega r^*),$$

where  $T(\omega)$  and  $R(\omega)$  are two unconstrained coefficients (these coefficients turn out to be the transmission and reflection coefficient; see section 4). Similarly,  $\phi_{\omega(0,1)}^*(r^*)$  is the radial function which at  $r^* \rightarrow -\infty$  has the asymptotic form

$$\phi_{\omega(0,1)}^* \cong T'(\omega)\exp(+i\omega r^*)$$

and at  $r^* \rightarrow +\infty$  has the asymptotic form

$$\phi_{\omega(0,1)}^* \cong \exp(+i\omega r^*) + R'(\omega)\exp(-i\omega r^*),$$

where again  $T'(\omega)$  and  $R'(\omega)$  are two unconstrained coefficients. Now, the two desired solutions  $\phi_{(\omega_v, 0)}^*$  and  $\phi_{(0, \omega_u)}^*$  are simply given by

$$\begin{aligned} \phi_{(\omega_v, 0)}^*(r^*, t) &= \phi_{\omega_v(1,0)}^*(r^*)\exp(i\omega_v t), \\ \phi_{(0, \omega_u)}^*(r^*, t) &= \phi_{\omega_u(0,1)}^*(r^*)\exp(i\omega_u t). \end{aligned}$$

As one can easily verify, these two solutions take the asymptotic forms

$$\phi_{(\omega_v,0)}^* \cong T(\omega_v)\exp(i\omega_v v) \quad (r^* \rightarrow +\infty),$$

$$\phi_{(\omega_v,0)}^* \cong \exp(i\omega_v v) + R(\omega)\exp(i\omega_v u) \quad (r^* \rightarrow -\infty),$$

and

$$\phi_{(0,\omega_u)}^* \cong T'(\omega_u)\exp(i\omega_u u) \quad (r^* \rightarrow -\infty),$$

$$\phi_{(0,\omega_u)}^* \cong \exp(i\omega_u u) + R'(\omega)\exp(i\omega_u v) \quad (r^* \rightarrow +\infty),$$

in agreement with the above definitions of  $\phi_{(\omega_v,0)}^*$  and  $\phi_{(0,\omega_u)}^*$ .

## D. Bessel functions

Let us assemble a few useful properties of the Bessel functions. A Bessel function of order  $n$  satisfies the equation  $[\partial_{xx} + (1/x)\partial_x + 1 - n^2/x^2]J_n = 0$ . It will be more convenient for us to use the equivalent definition

$$\left[ \partial_{xx} + \left( 1 - \frac{n^2 - 1/4}{x^2} \right) \right] \sqrt{x} J_n(x) = 0. \quad (\text{D.1})$$

For small  $x$

$$J_n(x) = x^n A_n^J(x^2), \quad (\text{D.2})$$

where  $A_n^J(x^2)$  are certain functions of  $x^2$  analytic at  $x^2 = 0$ . The asymptotic behavior is better described by

$$Y_n = (J_n \cos(n\pi) - J_{-n}) / \sin(n\pi) \quad (\text{D.3})$$

and one has

$$J_n \pm i Y_n \simeq \sqrt{2/(\pi x)} \exp[\pm i(x - n\pi/2 - \pi/4)] \quad (\text{D.4})$$

as  $x \rightarrow +\infty$ .

## References

- [1] J. Polchinski, “String Theory. Vol. 2: Superstring Theory And Beyond,” “String Theory. Vol. 1: An Introduction To The Bosonic String.”
- [2] A. Giveon, E. Rabinovici and A. Sever, “Strings in singular time-dependent backgrounds,” *Fortsch. Phys.* **51**, 805 (2003) [arXiv:hep-th/0305137].
- [3] R. Dijkgraaf, H. Verlinde and E. Verlinde, “String propagation in a black hole geometry,” *Nucl. Phys. B* **371** (1992) 269.
- [4] A. Giveon, E. Rabinovici and A. Sever, “Beyond the singularity of the 2-D charged black hole,” *JHEP* **0307**, 055 (2003) [arXiv:hep-th/0305140].
- [5] J. M. Bardeen, *Nature* **226** 64 (1970).
- [6] K. S. Thorne, *Astrophys. J.* **191** 507 (1974).
- [7] For a recent observation see R. Genzel, R. Schoedel, T. Ott, A. Eckart, T. Alexander, F. Lacombe, D. Rouan, B. Aschenbach, *Nature* **425**, 934 (2003).

- [8] A. Ishibashi and A. Hosoya, “Who’s afraid of naked singularities? Probing timelike singularities with finite energy waves,” *Phys. Rev. D* **60**, 104028 (1999) [arXiv:gr-qc/9907009].
- [9] R. M. Wald, “Dynamics in nonglobally hyperbolic, static space-times,” *J. Math. Phys.* **21**, 2802 (1980).
- [10] G. T. Horowitz and D. Marolf, “Quantum probes of space-time singularities,” *Phys. Rev. D* **52**, 5670 (1995) [arXiv:gr-qc/9504028].
- [11] K. Peeters, C. Schweigert and J. W. van Holten, “Extended geometry of black holes,” *Class. Quant. Grav.* **12**, 173 (1995) [arXiv:gr-qc/9407006].
- [12] T. Jacobson, “Semiclassical decay of near-extremal black holes,” *Phys. Rev. D* **57**, 4890 (1998) [arXiv:hep-th/9705017].
- [13] D. Lynden-Bell and J. Katz, “Geometric extension through Schwarzschild  $r = 0$ ,” *Mon. Not. Roy. Astron. Soc.* (1990) **247**, 651.
- [14] D. Lynden-Bell, J. Katz and C. Hellaby, “Correction to geometric extension through Schwarzschild  $r = 0$ ,” *Mon. Not. Roy. Astron. Soc.* (1993) **262**, 325.
- [15] H. Reissner, “Über die Eigengravitation des elektrischen Felds nach den Einsteinschen Theorie,” *Ann. Phys.* **50**, 106-120 (1916).
- [16] G. Nordström, “On the energy of the gravitational field in Einstein’s theory,” *Proc. Kon. Ned. Akad. Wet.* **20**, 1238-1245 (1918).
- [17] K. Schwarzschild, “Über das Gravitationsfeld eines Massenpunktes nach der Einsteinschen Theorie,” *Sitzber. Deut. Akad. Wiss. Berlin, Kl. Math.-Phys. Tech.* 189-196 (1916).  
English translation: *Gen. Relativ. Gravit.* **35**, 951 (2003) [physics/9905030].
- [18] M. D. Kruskal, “Maximal Extension Of Schwarzschild Metric,” *Phys. Rev.* **119**, 1743 (1960).
- [19] G. Szekeres, “On the singularities of a Riemannian manifold,” *Publ. Mat. Debrecen* **7**, 285-301, (1960).
- [20] W. Israel, “Singular Hypersurfaces And Thin Shells In General Relativity,” *Nuovo Cim. B* **44S10**, 1 (1966) [Erratum-ibid. *B* **48**, 463 (1967 NUCIA,B44,1.1966)].
- [21] M. Visser, “Traversable Wormholes From Surgically Modified Schwarzschild Space-Times,” *Nucl. Phys. B* **328**, 203 (1989).
- [22] T. Hertog, G. T. Horowitz, and K. Maeda, “Negative Energy in String Theory and Cosmic Censorship Violation”, hep-th/0310054.
- [23] R. Penrose, in *Battelle Rencontres, 1967 lectures in mathematics and physics*, edited by C. M. DeWitt and J. A. Wheeler (Benjamin, New York, 1968), P. 222 .
- [24] E. Poisson and W. Israel, “Internal Structure Of Black Holes,” *Phys. Rev. D* **41**, 1796 (1990) and references therein.
- [25] A. Ori, “Inner structure of a charged black hole: An exact mass-inflation solution,” *Phys. Rev. Lett.* **67**, 789 (1991).
- [26] L. M. Burko, “Structure of the black hole’s Cauchy horizon singularity,” *Phys. Rev. Lett.* **79**, 4958 (1997) [arXiv:gr-qc/9710112].

- [27] This is also the situation in the more realistic, spinning black-hole case: see e.g. A. Ori, “Structure of the singularity inside a realistic rotating black hole,” *Phys. Rev. Lett.* **68**, 2117 (1992); A. Ori, “Evolution Of Linear Gravitational And Electromagnetic Perturbations Inside A Kerr Black Hole,” *Phys. Rev. D* **61**, 024001 (2000).
- [28] L. D. Landau and E. M. Lifshitz, “Quantum mechanics,” *Pergamon* (1977), §35.
- [29] R. C. Myers and M. J. Perry, “Black holes in higher dimensional space-times,” *Annals Phys.* **172**, 304 (1986).
- [30] M. D. McGuigan, C. R. Nappi and S. A. Yost, “Charged black holes in two-dimensional string theory,” *Nucl. Phys. B* **375**, 421 (1992) [arXiv:hep-th/9111038].
- [31] I. Bars and K. Sfetsos, “Conformally exact metric and dilaton in string theory on curved space-time,” *Phys. Rev. D* **46** (1992) 4510 [arXiv:hep-th/9206006].
- [32] A. Giveon, “Target space duality and stringy black holes,” *Mod. Phys. Lett. A* **6**, 2843 (1991).
- [33] A. Giveon, M. Porrati and E. Rabinovici, “Target space duality in string theory,” *Phys. Rept.* **244**, 77 (1994) [arXiv:hep-th/9401139].
- [34] M. Reed and B. Simon, “Methods of modern mathematical physics, v2: Fourier analysis and self-adjointness”, *Academic Press* (1975).